CHAPTER 3
Crystalline Structure—Perfection

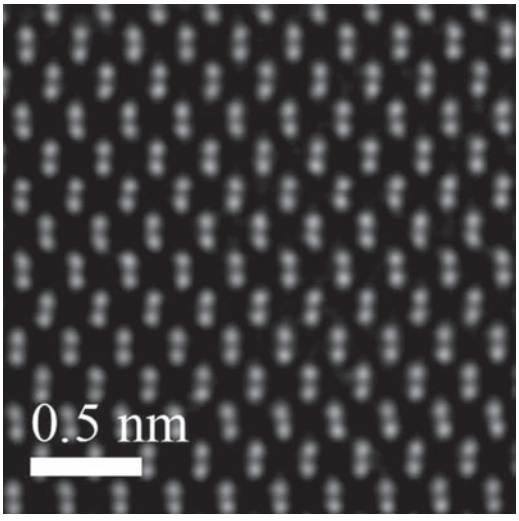

This high-resolution transmission electron micrograph illustrates the rhythmic arrangement of atoms in a silicon crystal. (Courtesy of Klaus van Benthem and Andrew Thron, University of California, Davis.)

With the categories of engineering materials firmly established, we can now begin characterizing these materials. We will begin with atomic-scale structure, which for most engineering materials is crystalline; that is, the atoms of the material are arranged in a regular and repeating manner.

Common to all crystalline materials are the fundamentals of crystal geometry. We must identify the seven crystal systems and the 14 crystal lattices. Each of the thousands of crystal structures found in natural and synthetic materials can be placed within these few systems and lattices.

The crystalline structures of most metals belong to one of three relatively simple types. Ceramic compounds, which have a wide variety of chemical compositions, exhibit a similarly wide variety of crystalline structures. Some are relatively simple, but many, such as the silicates, are quite complex. Glass is noncrystalline, and its structure and the nature of noncrystalline materials are discussed in Chapter 4. Polymers share two features with ceramics and glasses. First, their crystalline structures are relatively complex. Second, because of this complexity, the material is not easily crystallized, and common polymers may have as much as 50% to 100% of their volume noncrystalline. Elemental semiconductors, such as silicon, exhibit a characteristic structure (diamond cubic), whereas semiconducting compounds have structures similar to some of the simpler ceramic compounds.

Within a given structure, we must know how to describe atom positions, crystal directions, and crystal planes. With these quantitative ground rules in hand, we conclude this chapter with a brief introduction to x-ray diffraction, the standard experimental tool for determining crystal structure.

3.1 Seven Systems and Fourteen Lattices

The central feature of crystalline structure is that it is regular and repeating. In order to quantify this repetition, we must determine which structural unit is being repeated. Actually, any crystalline structure could be described as a pattern

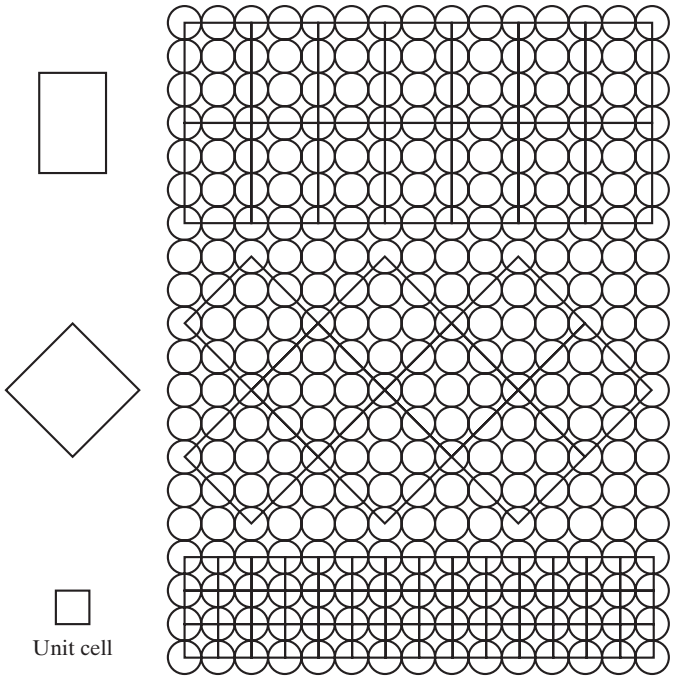

FIGURE 3.1 *Various structural units that describe the schematic crystalline structure. The simplest structural unit is the unit cell.*

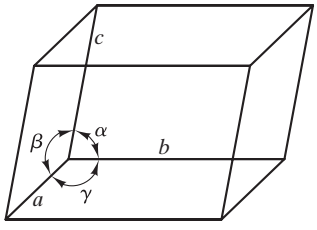

FIGURE 3.2 *Geometry of a general unit cell.*

formed by repeating various structural units (Figure 3.1). As a practical matter, there will generally be a simplest choice to serve as a representative structural unit. Such a choice is referred to as a **unit cell**. The geometry of a general unit cell is shown in Figure 3.2. The length of unit-cell edges and the angles between crystallographic axes are referred to as **lattice constants**, or **lattice parameters**. The key feature of the unit cell is that it contains a full description of the structure as a whole because the complete structure can be generated by the repeated stacking of adjacent unit cells face to face throughout three-dimensional space.

The description of crystal structures by means of unit cells has an important advantage. All possible structures reduce to a small number of basic unit-cell geometries, which is demonstrated in two ways. First, there are only seven unique unit-cell shapes that can be stacked together to fill three-dimensional space. These are the seven **crystal systems** defined and illustrated in Table 3.1. Second, we must consider how atoms (viewed as hard spheres) can be stacked together within a given unit cell. To do this in a general way, we begin by considering **lattice points**, theoretical points arranged periodically in three-dimensional space, rather than actual atoms or spheres. Again, there are a limited number of possibilities, referred to as the 14 **Bravais*** **lattices**, defined in Table 3.2. Periodic stacking of unit cells from Table 3.2 generates **point lattices**, arrays of points with identical surroundings in three-dimensional space. These lattices are skeletons

*Auguste Bravais (1811–1863), French crystallographer, was productive in an unusually broad range of areas, including botany, astronomy, and physics. However, it is his derivation of the 14 possible arrangements of points in space that is best remembered. This achievement provided the foundation for our current understanding of the atomic structure of crystals.

TABLE 3.1

The Seven Crystal Systems

System	Axial lengths and angles[a]	Unit cell geometry
Cubic	$a = b = c,\ \alpha = \beta = \gamma = 90°$	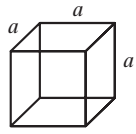
Tetragonal	$a = b \neq c,\ \alpha = \beta = \gamma = 90°$	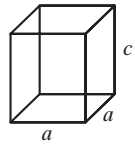
Orthorhombic	$a \neq b \neq c,\ \alpha = \beta = \gamma = 90°$	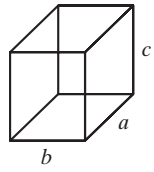
Rhombohedral	$a = b = c,\ \alpha = \beta = \gamma \neq 90°$	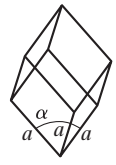
Hexagonal	$a = b \neq c,\ \alpha = \beta = 90°,\ \gamma = 120°$	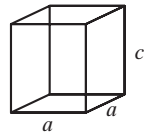
Monoclinic	$a \neq b \neq c,\ \alpha = \gamma = 90° \neq \beta$	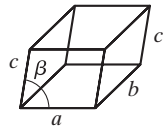
Triclinic	$a \neq b \neq c,\ \alpha \neq \beta \neq \gamma \neq 90°$	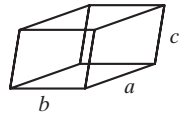

[a]The lattice parameters a, b, and c are unit-cell edge lengths. The lattice parameters α, β, and γ are angles between adjacent unit-cell axes, where α is the angle viewed along the a axis (i.e., the angle between the b and c axes). The inequality sign ($\neq$) means that equality is not required. Accidental equality occasionally occurs in some structures.

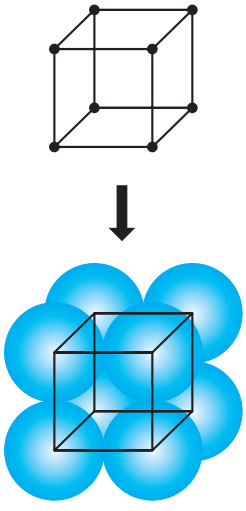

FIGURE 3.3 *The simple cubic lattice becomes the simple cubic crystal structure when an atom is placed on each lattice point.*

upon which crystal structures are built by placing atoms or groups of atoms on or near the lattice points. Figure 3.3 shows the simplest possibility, with one atom centered on each lattice point. Some of the simple metal structures are of this type. However, a very large number of actual crystal structures is known to exist.

TABLE 3.2

The 14 Crystal (Bravais) Lattices

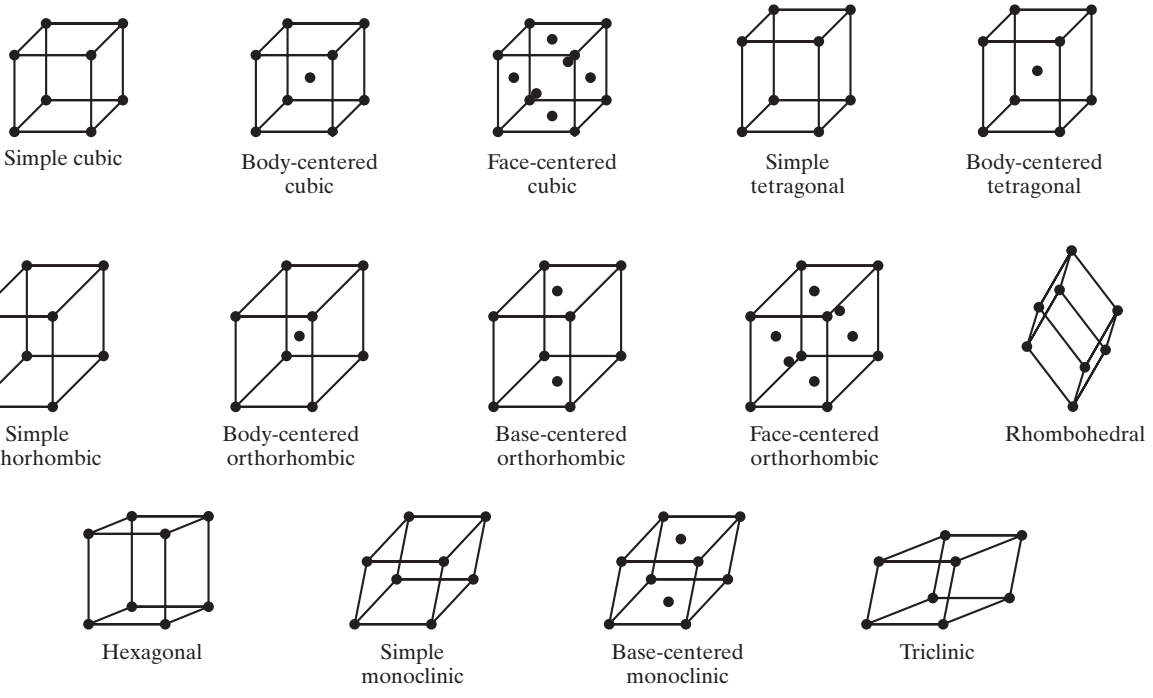

Most of these structures result from having more than one atom associated with a given lattice point. We shall find many examples in the crystal structures of common ceramics and polymers (Sections 3.3 and 3.4).

EXAMPLE 3.1

Sketch the five point lattices for two-dimensional crystal structures.

SOLUTION

Unit-cell geometries are (i) simple square, (ii) simple rectangle, (iii) area-centered rectangle (or rhombus), (iv) parallelogram, and (v) area-centered hexagon.

Note. It is a useful exercise to construct other possible geometries that must be equivalent to these five basic types. For example, an area-centered square can be resolved into a simple square lattice (inclined at 45°).

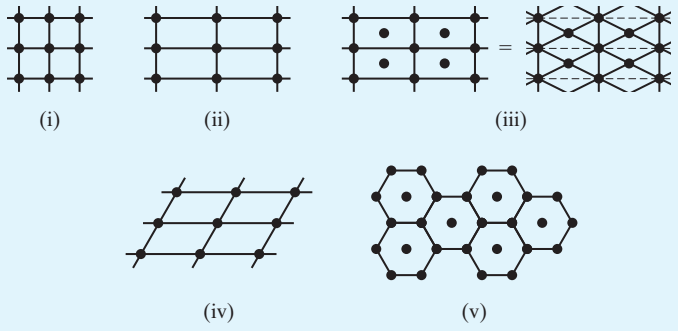

PRACTICE PROBLEM 3.1

The note in Example 3.1 states that an area-centered square lattice can be resolved into a simple square lattice. Sketch this equivalence.

3.2 Metal Structures

With the structural ground rules behind us, we can now list the main crystal structures associated with important engineering materials. For our first group, the metals, this list is fairly simple. As we see from an inspection of Appendix 1, most elemental metals at room temperature are found in one of three crystal structures.

Figure 3.4 shows the **body-centered cubic** (bcc) structure, which is the body-centered cubic **Bravais lattice** with one atom centered on each lattice point. There is one atom at the center of the unit cell and one-eighth atom at each of eight unit-cell corners. (Each corner atom is shared by eight adjacent unit cells.) Thus, there are two atoms in each bcc unit cell. The **atomic packing factor (APF)** for this structure is 0.68 and represents the fraction of the unit-cell volume occupied by the two atoms. Typical metals with this structure include α-Fe (the form stable at room temperature), V, Cr, Mo, and W. An alloy in which one of these metals is the predominant constituent will tend to have this structure also. However, the presence of alloying elements diminishes crystalline perfection, a topic that will be discussed in Chapter 4.

Figure 3.5 shows the **face-centered cubic** (fcc) structure, which is the fcc Bravais lattice with one atom per lattice point. There is one-half atom (i.e., one atom shared between two unit cells) in the center of each unit-cell face and one-eighth atom at each unit-cell corner, for a total of four atoms in each fcc unit cell. The atomic packing factor for this structure is 0.74, a value slightly higher than the 0.68 found for bcc metals. In fact, an APF of 0.74 is the highest value possible for filling space by stacking equal-sized hard spheres. For this reason, the fcc structure is sometimes referred to as **cubic close packed** (ccp). Typical metals with the fcc structure include γ-Fe (stable from 912 to 1,394°C), Al, Ni, Cu, Ag, Pt, and Au.

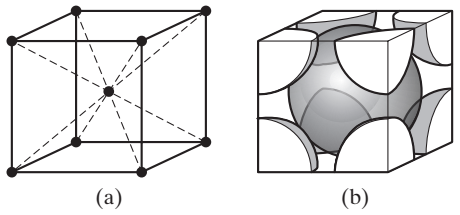

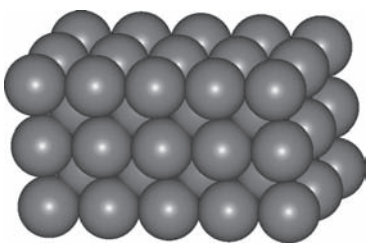

Structure: body-centered cubic (bcc)
Bravais lattice: bcc
Atoms/unit cell: $1 + 8 \times \frac{1}{8} = 2$
Typical metals: α-Fe, V, Cr, Mo, and W

FIGURE 3.4 *Body-centered cubic (bcc) structure for metals showing (a) the arrangement of lattice points for a unit cell, (b) the actual packing of atoms (represented as hard spheres) within the unit cell, and (c) the repeating bcc structure, equivalent to many adjacent unit cells. [Part (c) courtesy of Accelrys, Inc.]*

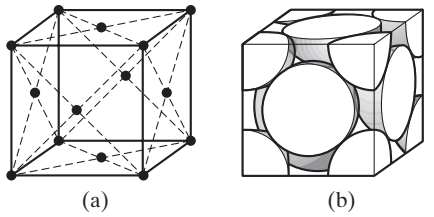

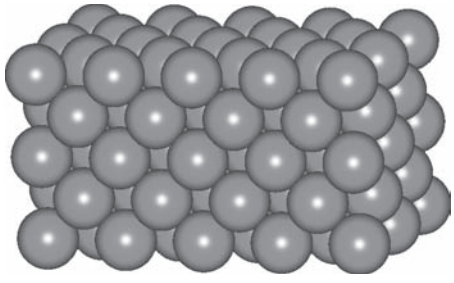

Structure: face-centered cubic (fcc)
Bravais lattice: fcc
Atoms/unit cell: $6 \times \frac{1}{2} + 8 \times \frac{1}{8} = 4$
Typical metals: γ-Fe, Al, Ni, Cu, Ag, Pt, and Au

FIGURE 3.5 *Face-centered cubic (fcc) structure for metals showing (a) the arrangement of lattice points for a unit cell, (b) the actual packing of atoms within the unit cell, and (c) the repeating fcc structure, equivalent to many adjacent unit cells. [Part (c) courtesy of Accelrys, Inc.]*

The **hexagonal close-packed** (hcp) structure (Figure 3.6) is our first encounter with a structure more complicated than its Bravais lattice (hexagonal). There are two atoms associated with each Bravais lattice point. There is one atom centered within the unit cell and various fractional atoms at the unit-cell corners (four $\frac{1}{6}$ atoms and four $\frac{1}{12}$ atoms), for a total of two atoms per unit cell. As the *close-packed* name implies, this structure is as efficient in packing spheres as is the fcc structure. Both hcp and fcc structures have atomic packing factors of 0.74, which raises two questions: (1) In what other ways are the fcc and hcp structures alike? and (2) How do they differ? The answers to both questions can be found in Figure 3.7. The two structures are each regular stackings of close-packed planes. The difference lies in the sequence of packing of these layers. The fcc arrangement is such that the fourth close-packed layer lies precisely above the first one. In the hcp structure, the third close-packed layer lies precisely above the first. The fcc stacking is referred to as an *ABCABC . . . sequence,* and the hcp stacking is referred to as an *ABAB . . . sequence*. This subtle difference can lead to significant differences in material properties, as we shall see in Section 6.3. Typical metals with the hcp structure include Be, Mg, α-Ti, Zn, and Zr.

Although the majority of elemental metals fall within one of the three structural groups just discussed, several display less common structures. We shall not dwell on these cases, which can be found from a careful inspection of Appendix 1.

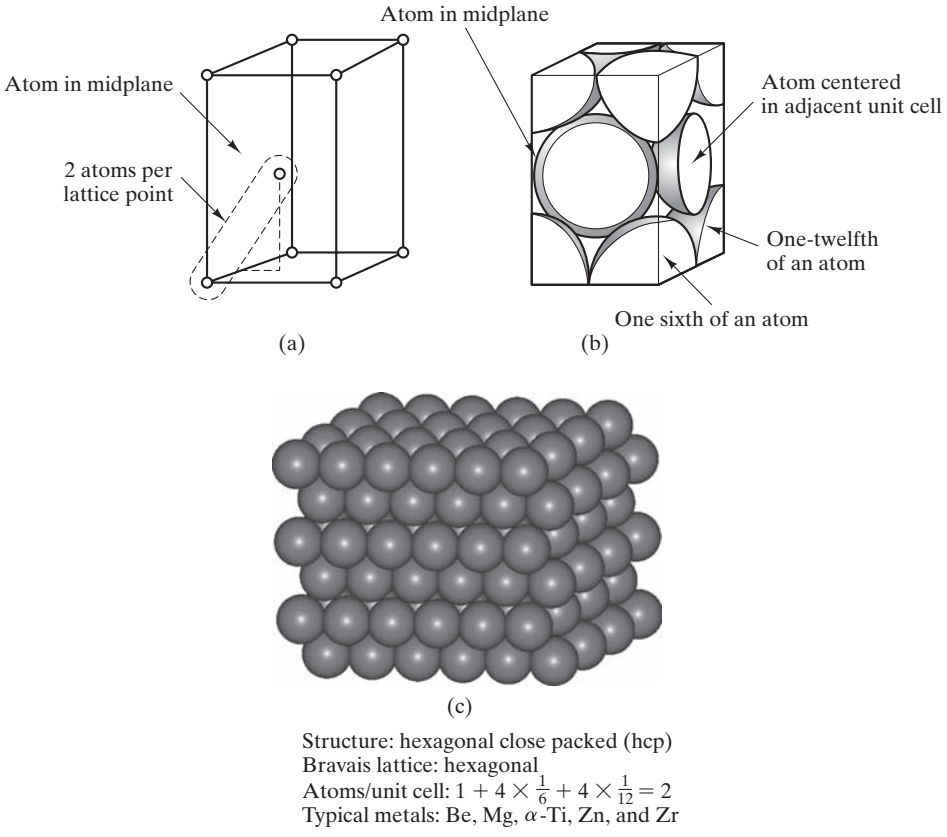

FIGURE 3.6 *Hexagonal close-packed (hcp) structure for metals showing (a) the arrangement of atom centers relative to lattice points for a unit cell. There are two atoms per lattice point (note the outlined example). (b) The actual packing of atoms within the unit cell. Note that the atom in the midplane extends beyond the unit-cell boundaries. (c) The repeating hcp structure, equivalent to many adjacent unit cells. [Part (c) courtesy of Accelrys, Inc.]*

In the course of analyzing the metallic structures introduced in this section, we shall frequently encounter the useful relationships between unit-cell size and atomic radius given in Table 3.3. Our initial discovery of the utility of these relationships is found in the following examples and practice problems.

TABLE 3.3

Relationship between Unit-Cell Size (Edge Length) and Atomic Radius for the Common Metallic Structures

Crystal structure	Relationship between edge length, a, and atomic radius, r
Body-centered cubic (bcc)	$a = 4r/\sqrt{3}$
Face-centered cubic (fcc)	$a = 4r/\sqrt{2}$
Hexagonal close packed (hcp)	$a = 2r$

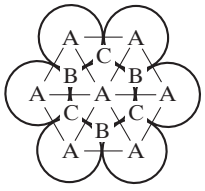

(a) Stacking of close-packed planes

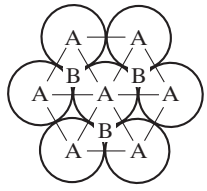

(b) Stacking of close-packed planes

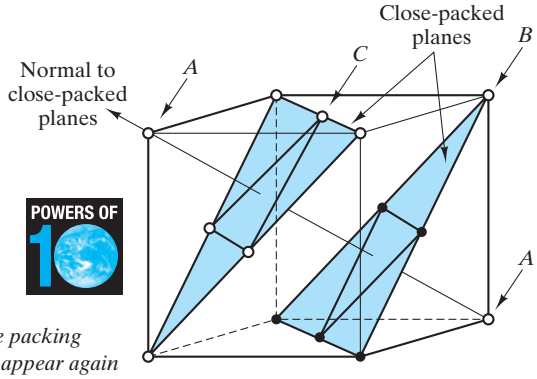

(c) Face-centered cubic

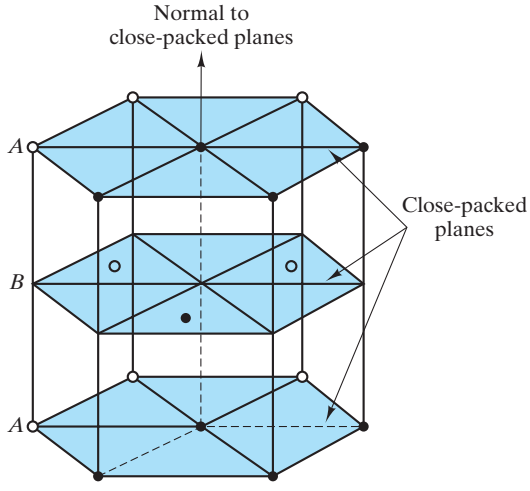

(d) Hexagonal close packed

These atomic scale packing arrangements will appear again in Table 6.8, central to our understanding of the plastic deformation of metals.

FIGURE 3.7 *Comparison of the fcc and hcp structures. They are each efficient stackings of close-packed planes. The difference between the two structures is the different stacking sequences. (From B. D. Cullity and S. R. Stock,* Elements of X-Ray Diffraction*, 3rd ed., Prentice-Hall, Upper Saddle River, NJ, 2001.)*

EXAMPLE 3.2

Using the data of Appendices 1 and 2, calculate the density of copper.

SOLUTION

Appendix 1 shows copper to be an fcc metal. The length, l, of a face diagonal in the unit cell (Figure 3.5) is

$$l = 4r_{\text{Cu atom}} = \sqrt{2}a$$

or

$$a = \frac{4}{\sqrt{2}} r_{\text{Cu atom}},$$

as given in Table 3.3. From the data of Appendix 2,

$$a = \frac{4}{\sqrt{2}}(0.128\ \text{nm}) = 0.362\ \text{nm}.$$

The density of the unit cell (containing four atoms) is

$$\rho = \frac{4 \text{ atoms}}{(0.362 \text{ nm})^3} \times \frac{63.55\ g}{0.6023 \times 10^{24} \text{ atoms}} \times \left(\frac{10^7 \text{ nm}}{\text{cm}}\right)^3$$

$$= 8.89 \text{ g/cm}^3.$$

This result can be compared with the tabulated value of 8.93 g/cm^3 in Appendix 1. The difference would be eliminated if a more precise value of $r_{\text{Cu atom}}$ were used (i.e., with at least one more significant figure).

PRACTICE PROBLEM 3.2

In Example 3.2, the relationship between lattice parameter, *a,* and atomic radius, *r,* for an fcc metal is found to be $a = (4/\sqrt{2})r$, as given in Table 3.3. Derive the similar relationships in Table 3.3 for **(a)** a bcc metal and **(b)** an hcp metal.

PRACTICE PROBLEM 3.3

Calculate the density of α-Fe, which is a bcc metal. (*Caution:* A different relationship between lattice parameter, *a,* and atomic radius, *r,* applies to this different crystal structure. See Practice Problem 3.2 and Table 3.3.)

3.3 Ceramic Structures

The wide variety of chemical compositions of ceramics is reflected in their crystalline structures. We cannot begin to give an exhaustive list of ceramic structures, but we can give a systematic list of some of the most important and representative ones. Even this list becomes rather long, so most structures will be described briefly. It is worth noting that many of these ceramic structures also describe intermetallic compounds. Also, we can define an **ionic packing factor** (IPF) for these ceramic structures, similar to our definition of the APF for metallic structures. The IPF is the fraction of the unit-cell volume occupied by the various cations and anions.

Let us begin with the ceramics with the simplest chemical formula, MX, where M is a metallic element and X is a nonmetallic element. Our first example is the **cesium chloride** (CsCl) structure shown in Figure 3.8. At first glance, we might want to call this a body-centered structure because of its similarity in appearance to the structure shown in Figure 3.4. In fact, the CsCl structure is built on the simple cubic Bravais lattice with two ions (one Cs^+ and one Cl^-) associated with each lattice point. There are two ions (one Cs^+ and one Cl^-) per unit cell.

Although CsCl is a useful example of a compound structure, it does not represent any commercially important ceramics. By contrast, the **sodium chloride** (NaCl) structure shown in Figure 3.9 is shared by many important ceramic materials. This structure can be viewed as the intertwining of two fcc structures, one of sodium ions and one of chlorine ions. Consistent with our treatment of the hcp and CsCl structures, the NaCl structure can be described as having an fcc Bravais lattice with two ions (1 $Na^+$and 1 Cl^-) associated with each lattice

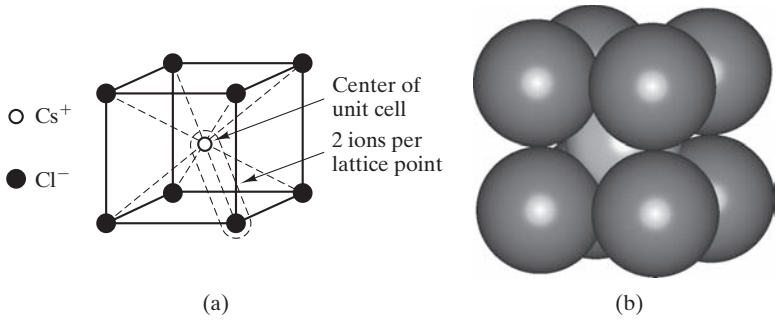

Structure: CsCl type
Bravais lattice: simple cubic
Ions/unit cell: $1Cs^+ + 1Cl^-$

FIGURE 3.8 *Cesium chloride (*CsCl*) unit cell showing (a) ion positions and the two ions per lattice point and (b) full-size ions. Note that the* $Cs^+ - Cl^-$ *pair associated with a given lattice point is not a molecule because the ionic bonding is nondirectional and because a given* Cs^+ *is equally bonded to eight adjacent* Cl^-*, and vice versa. [Part (b) courtesy of Accelrys, Inc.]*

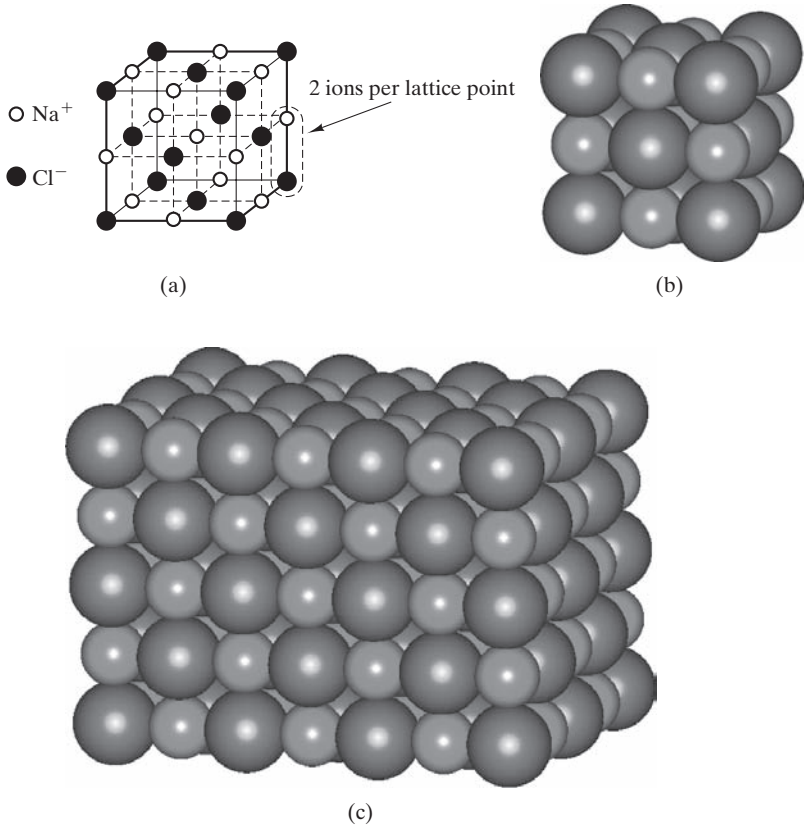

Structure: NaCl type
Bravais lattice: fcc
Ions/unit cell: $4Na^+ + 4Cl^-$
Typical ceramics: MgO, CaO, FeO, and NiO

FIGURE 3.9 *Sodium chloride (*NaCl*) structure showing (a) ion positions in a unit cell, (b) full-size ions, and (c) many adjacent unit cells. [Parts (b) and (c) courtesy of Accelrys, Inc.]*

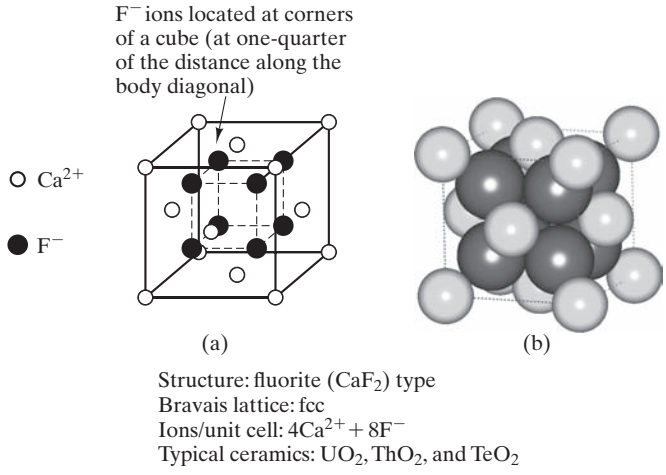

FIGURE 3.10 *Fluorite (CaF_2) unit cell showing (a) ion positions and (b) full-size ions. [Part (b) courtesy of Accelrys, Inc.]*

point. There are eight ions (4 Na^+ plus 4 Cl^-) per unit cell. Some of the important ceramic oxides with this structure are MgO, CaO, FeO, and NiO.

The chemical formula MX_2 includes a number of important ceramic structures. Figure 3.10 shows the **fluorite** (CaF_2) structure, which is built on an fcc Bravais lattice with three ions (1 Ca^{2+} and 2F^-) associated with each lattice point. There are 12 ions (4 Ca^{2+} and 8 F^-) per unit cell. Typical ceramics with this structure are UO_2, ThO_2, and TeO_2. There is an unoccupied volume near the center of the fluorite unit cell that plays an important role in nuclear-materials technology. Uranium dioxide (UO_2) is a reactor fuel that can accommodate fission products such as helium gas without troublesome swelling. The helium atoms are accommodated in the open regions of the fluorite unit cells.

Included in the MX_2 category is perhaps the most important ceramic compound, **silica** (SiO_2), which is widely available in raw materials in the earth's crust. Silica, alone and in chemical combination with other ceramic oxides (forming silicates), represents a large fraction of the ceramic materials available to engineers. For this reason, the structure of SiO_2 is important. Unfortunately, this structure is not simple. In fact, there is not a single structure to describe it, but instead there are many (under different conditions of temperature and pressure). For a representative example, Figure 3.11 shows the **cristobalite** (SiO_2) structure. Cristobalite is built on an fcc Bravais lattice with six ions (2 Si^{4+} and 4 O^{2-}) associated with each lattice point. There are 24 ions (8 Si^{4+} plus 16 O^{2-}) per unit cell. In spite of the large unit cell needed to describe this structure, it is perhaps the simplest of the various crystallographic forms of SiO_2. The general feature of all SiO_2 structures is the same—a continuously connected network of SiO_4^{4-} tetrahedra (see Section 2.3). The sharing of O^{2-} ions by adjacent tetrahedra gives the overall chemical formula SiO_2.

We have already noticed (in Section 3.2) that iron, Fe, had different crystal structures stable in different temperature ranges. The same is true for silica, SiO_2. Although the basic SiO_4^{4-} tetrahedra are present in all SiO_2 crystal structures, the arrangement of connected tetrahedra changes. The equilibrium structures of SiO_2 from room temperature to its melting point are summarized in Figure 3.12. Caution must always be exercised in using materials with transformations of these types.

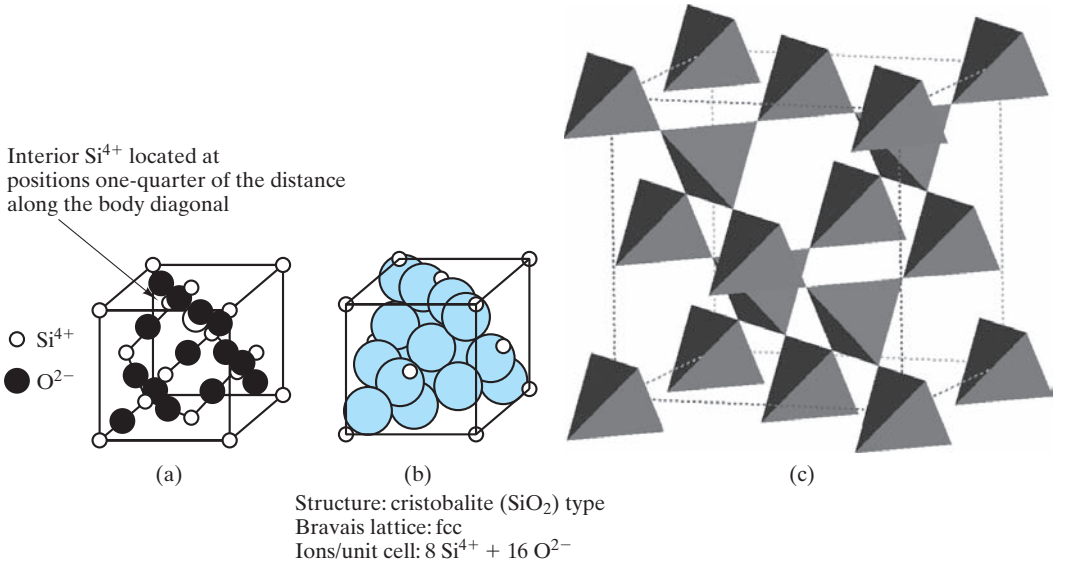

FIGURE 3.11 *The cristobalite (SiO_2) unit cell showing (a) ion positions, (b) full-size ions, and (c) the connectivity of SiO_4^{4-} tetrahedra. In the schematic, each tetrahedron has a Si^{4+} at its center. In addition, an O^{2-} would be at each corner of each tetrahedron and is shared with an adjacent tetrahedron. [Part (c) courtesy of Accelrys, Inc.]*

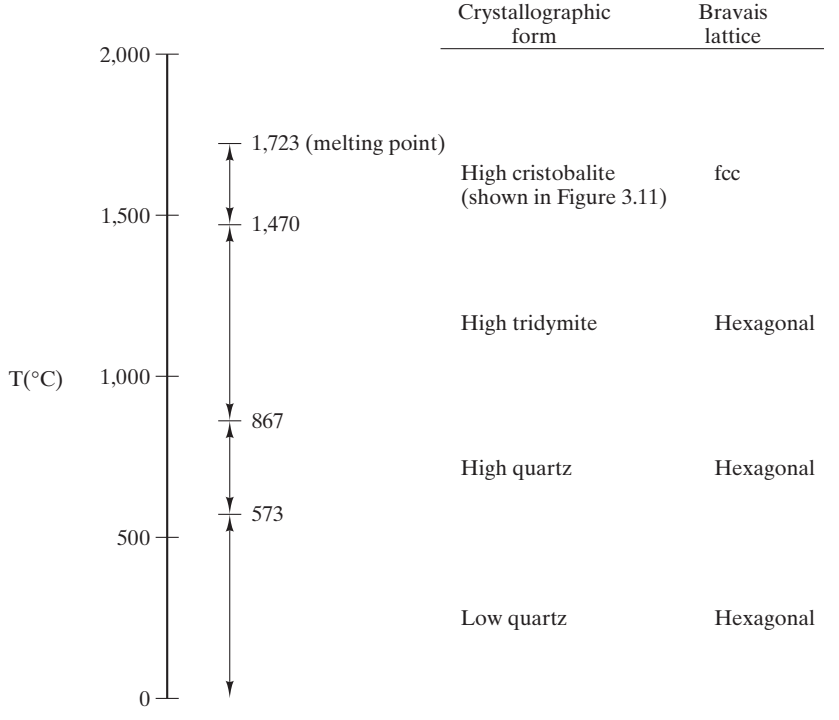

FIGURE 3.12 *Many crystallographic forms of SiO_2 are stable as they are heated from room temperature to melting temperature. Each form represents a different way to connect adjacent SiO_4^{4-} tetrahedra.*

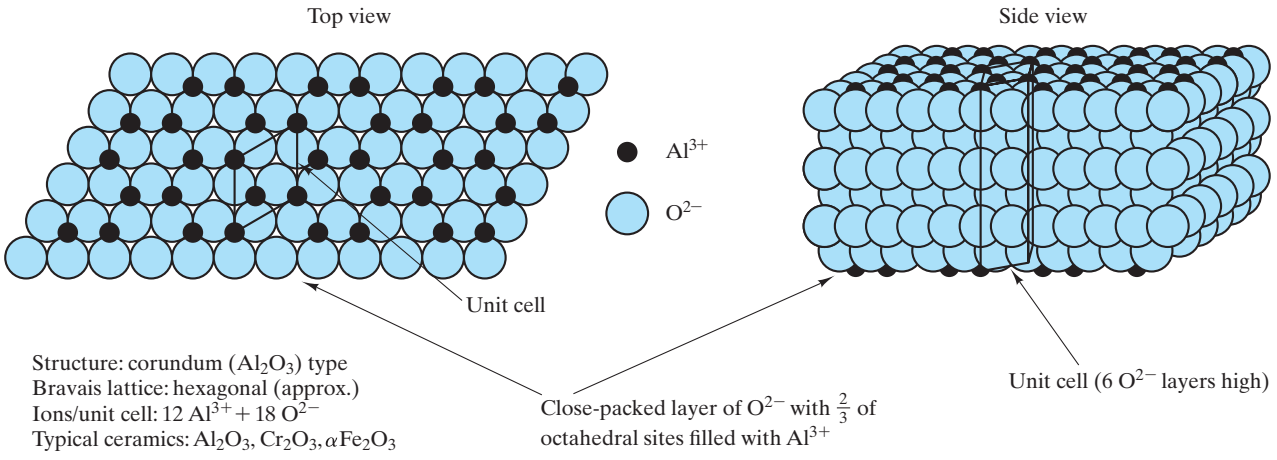

FIGURE 3.13 *The corundum* (Al_2O_3) *unit cell is shown superimposed on the repeated stacking of layers of close-packed* O^{2-} *ions. The* Al^{3+} *ions fill two-thirds of the small (octahedral) interstices between adjacent layers.*

Even the relatively subtle low to high quartz transformation can cause catastrophic structural damage when a silica ceramic is heated or cooled through the vicinity of 573°C.

The chemical formula M_2X_3 includes the important **corundum** (Al_2O_3) structure shown in Figure 3.13. This structure is in a rhombohedral Bravais lattice, but it closely approximates a hexagonal lattice. There are 30 ions per lattice site (and per unit cell). The Al_2O_3 formula requires that these 30 ions be divided as 12 Al^{3+} and 18 O^{2-}. One can visualize this seemingly complicated structure as being similar to the hcp structure described in Section 3.2. The Al_2O_3 structure closely approximates close-packed O^{2-} sheets with two-thirds of the small interstices between sheets filled with Al^{3+}. Both Cr_2O_3 and α-Fe_2O_3 have the corundum structure.

In discussing the complexity of the SiO_2 structures, we mentioned the importance of the many silicate materials resulting from the chemical reaction of SiO_2 with other ceramic oxides. The general nature of silicate structures is that the additional oxides tend to break up the continuity of the SiO_4^{4-} tetrahedra connections. The remaining connectedness of tetrahedra may be in the form of silicate chains or sheets. One relatively simple example is illustrated in Figure 3.14, which shows the **kaolinite** structure. Kaolinite [$2(OH)_4Al_2Si_2O_5$] is a hydrated aluminosilicate and a good example of a clay mineral. The structure is typical of sheet silicates. It is built on the triclinic Bravais lattice with two kaolinite "molecules" per unit cell. On a microscopic scale, we observe many clay minerals to have a platelike or flaky structure (see Figure 3.15), a direct manifestation of crystal structures such as those shown in Figure 3.14.

In this section, we have surveyed crystal structures for various ceramic compounds. The structures have generally been increasingly complex as we considered increasingly complex chemistry. The contrast between CsCl (Figure 3.8) and kaolinite (Figure 3.14) is striking.

Before leaving ceramics, it is appropriate to look at some important materials that are exceptions to our general description of ceramics as compounds. First,

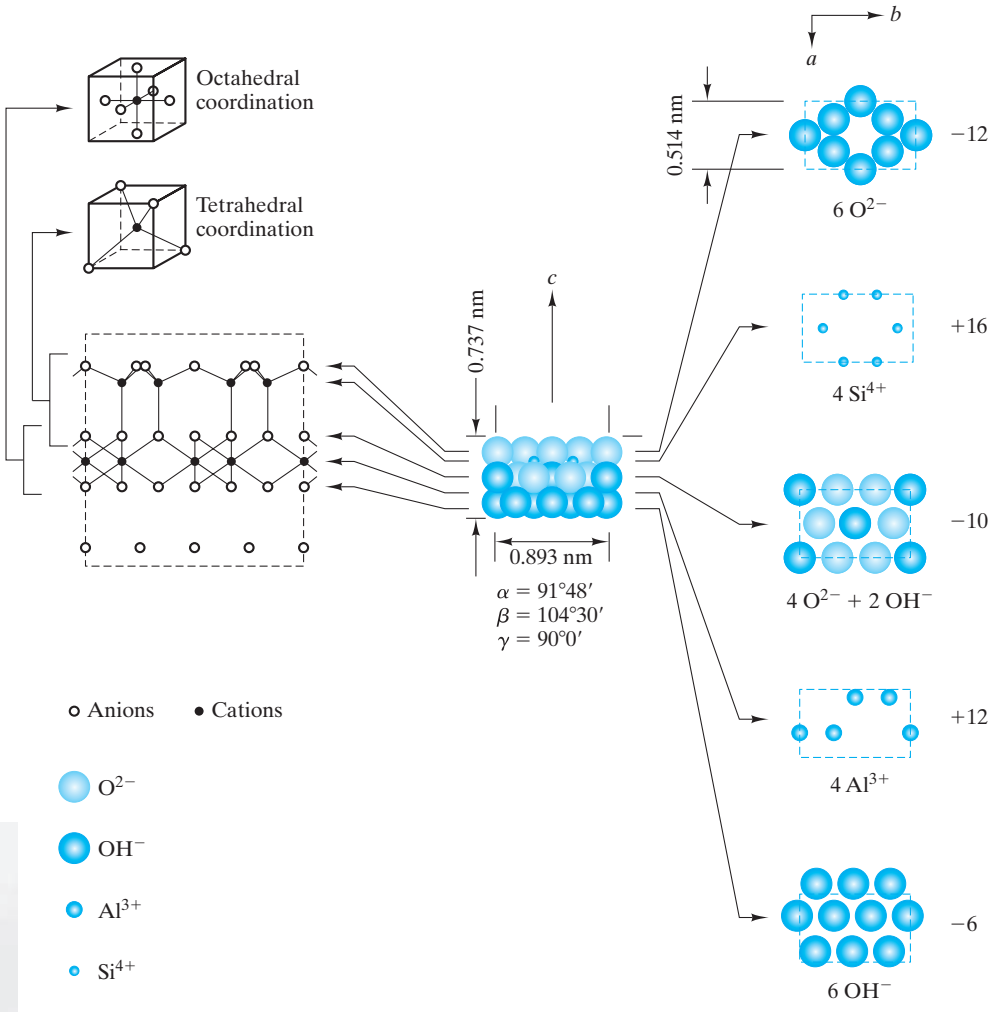

FIGURE 3.14 *Exploded view of the kaolinite unit cell,* $2(OH)_4Al_2Si_2O_5$. *(From F. H. Norton,* Elements of Ceramics, *2nd ed., Addison-Wesley Publishing Co., Inc., Reading, MA, 1974.)*

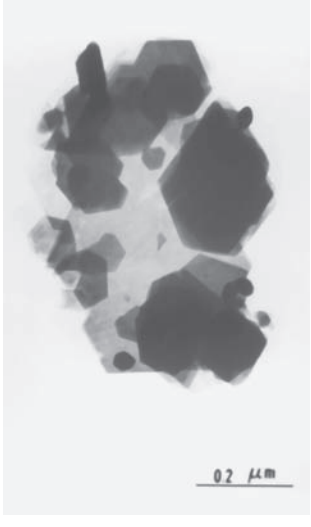

FIGURE 3.15 *Transmission electron micrograph of the structure of clay platelets. This microscopic-scale structure is a manifestation of the layered crystal structure shown in Figure 3.14. (Courtesy of I. A. Aksay.)*

Figure 3.16 shows the layered crystal structure of graphite, the stable room temperature form of carbon. Although monatomic, graphite is much more ceramic-like than metallic, the hexagonal rings of carbon atoms are strongly bonded by covalent bonds. The bonds between layers are, however, of the van der Waals type (Section 2.5), accounting for graphite's friable nature and application as a useful "dry" lubricant. It is interesting to contrast the graphite structure with the high-pressure stabilized form, diamond cubic, which plays such an important role in solid-state technology because semiconductor silicon has this structure (see Figure 3.20).

Even more intriguing is a comparison of both graphite and diamond structures with an alternate form of carbon that was discovered in the 1980s as a byproduct of research in astrochemistry. Figure 3.17(a) illustrates the structure of a C_{60} molecule. This unique structure was discovered during experiments on the laser vaporization of carbon in a carrier gas such as helium. The experiments had intended to simulate the synthesis of carbon chains in carbon stars. The

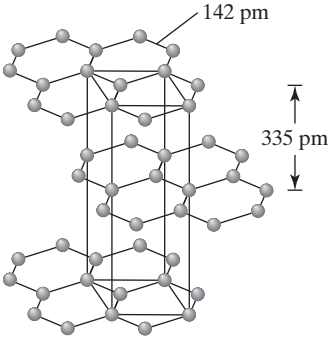

FIGURE 3.16 *A detailed view of the graphite (C) unit cell. (From Petrucci, R. H., F. G. Herring, J. D. Madura, and C. Bissonnette,* General Chemistry—Principles and Modern Applications with Mastering Chemistry®*, 10th ed., Prentice-Hall, Upper Saddle River, NJ, 2011.)*

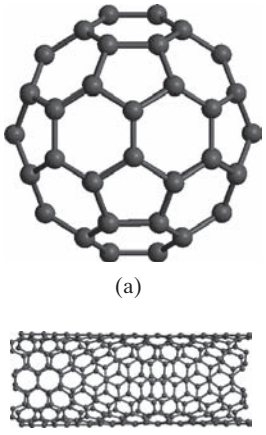

FIGURE 3.17 *(a) C_{60} molecule, or buckyball. (b) Cylindrical array of hexagonal rings of carbon atoms, or buckytube. (Courtesy of Accelrys, Inc.)*

result, however, was a molecular-scale version of the geodesic dome, leading to this material's being named **buckminsterfullerene**,* or **fullerene**, in honor of the inventor of that architectural structure. A close inspection of the structure shown in Figure 3.17(a) indicates that the nearly spherical molecule is, in fact, a polyhedron composed of 5- and 6-sided faces.

The uniform distribution of 12 pentagons among 20 hexagons is precisely the form of a soccer ball, leading to the nickname for the structure as a **buckyball**. It is the presence of 5-membered rings that gives the positive curvature to the surface of the buckyball, in contrast to the flat, sheetlike structure of 6-membered rings in graphite (Figure 3.16). Subsequent research has led to the synthesis of a wide variety of structures for a wide range of fullerenes. Buckyballs have been synthesized with the formula C_n, where n can take on various large, even values, such as 240 and 540. In each case, the structure consists of 12 uniformly distributed pentagons connecting an array of hexagons. Although pentagons are necessary to give the approximately spherical curvature of the buckyballs, extensive research on these unique materials led to the realization that cylindrical curvature can result from simply rolling the hexagonal graphite sheets. A resulting **buckytube** is shown in Figure 3.17(b).

These materials have stimulated enormous interest in the fields of chemistry and physics, as well as the field of materials science and engineering. Their molecular structure is clearly interesting, but in addition they have unique chemical and physical properties (e.g., individual C_n buckyballs are unique, passive surfaces on an nm-scale). Similarly, buckytubes hold the theoretical promise of being the highest-strength reinforcing fibers available for the advanced composites discussed in Chapter 12. These structures are the focus of substantial research

POWERS OF 10

The buckyball is helpful in appreciating the size of the "nanoscale." The ratio of the diameter of the earth to a soccer ball (that has the same geometrical distribution of pentagons and hexagons as the buckyball) is the same as the ratio of the diameter of the soccer ball to the buckyball (about 10^8 in both cases!).

*Richard Buckminster Fuller (1895–1983), American architect and inventor, was one of the most colorful and famous personalities of the 20th century. His creative discussions of a wide range of topics from the arts to the sciences (including frequent references to future trends) helped to establish his fame. In fact, his charismatic personality became as celebrated as his unique inventions of various architectural forms and engineering designs.

and development and are generally referred to as **carbon nanotubes** (CNT). The increasingly wide use of CNT in nanotechnology is discussed in the Feature Box in Chapter 15. Finally, we must acknowledge that the discrete molecular structures shown in Figure 3.17 are interesting but are not associated with a long range crystallographic structure. Nonetheless, buckyballs and buckytubes have an intriguing set of atomic-scale structures that could lead to potentially important applications in materials technology.

Within the past decade carbon materials again became the source of a major scientific discovery–**graphene**. As illustrated in Figure 3.18, graphene is simply a single atomic layer of graphite (compare with Figure 3.16). An experiment of astonishing simplicity produced this intriguing material. Researchers laid a piece of tape on top of graphite and pulled off a single layer of carbon atoms in the familiar hexagonal graphitic array. Although graphene had been known for decades and observed in a few esoteric environments, synthesis had eluded scientists until the now famous "scotch tape" experiment. The binding energy of the graphene layer to the adhesive tape was stronger than the van der Waals bonding between layers, allowing the single layer separation. This pathway to an abundant amount of graphene has led to an explosion of research and development efforts in both exploring other fabrication technologies and considering the technological possibilities of this unique material. This single atomic-layer material is exceptionally strong. An intriguing example is that, if one could produce a one-meter square "fabric" of graphene, a hammock made of the material could support the weight of a 4-kg cat while weighing only as much as one of the cat's whiskers. Graphene's electrical properties provide the potential for the increasing miniaturization of integrated circuits. Its high conductivity combined with high optical transparency suggests the potential for transparent conducting electrodes. With the high level of research effort currently devoted to graphene, the technological possibilities are as intriguing as they are not yet fully known.

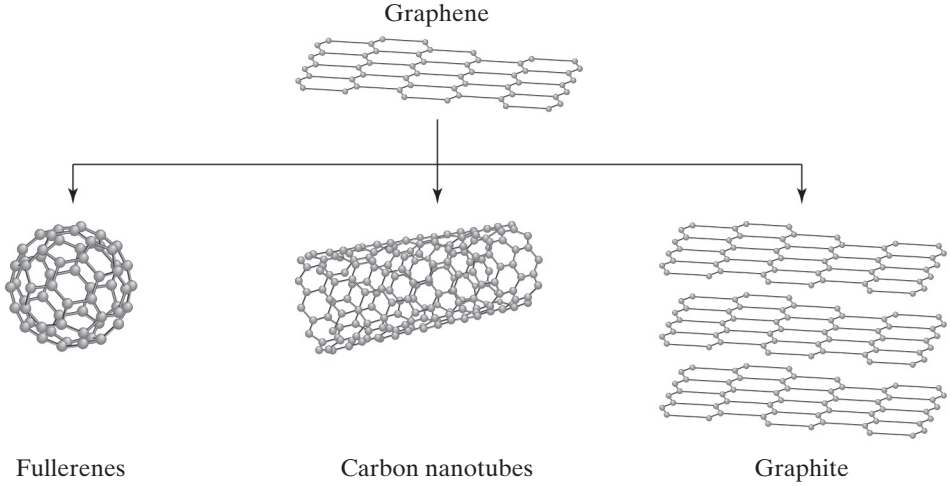

FIGURE 3.18 *Graphene is seen to be equivalent to a single graphite layer (compare to Figure 3.16) and an unrolled carbon nanotube [or buckytube as shown in Figure 3.17(b)]. (From Petrucci, R. H., F. G. Herring, J. D. Madura, and C. Bissonnette,* General Chemistry—Principles and Modern Applications with Mastering Chemistry®, *10th ed., Prentice-Hall, Upper Saddle River, NJ, 2011.)*

EXAMPLE 3.3

Calculate the IPF of MgO, which has the NaCl structure (Figure 3.9).

SOLUTION

Taking $a = 2r_{Mg^{2+}} + 2r_{O^{2-}}$ and the data of Appendix 2, we have

$$a = 2(0.078\ \text{nm}) + 2(0.132\ \text{nm}) = 0.420\ \text{nm}.$$

Then,

$$V_{\text{unit cell}} = a^3 = (0.420\ \text{nm})^3 = 0.0741\ \text{nm}^3.$$

There are four Mg^{2+} ions and four O^{2-} ions per unit cell, giving a total ionic volume of

$$\begin{aligned} &4 \times \frac{4}{3}\pi r^3_{Mg^{2+}} + 4 \times \frac{4}{3}\pi r^3_{O^{2-}} \\ &= \frac{16\pi}{3}[(0.078\ \text{nm})^3 + (0.132\ \text{nm})^3] \\ &= 0.0465\ \text{nm}^3. \end{aligned}$$

The ionic packing factor is then

$$\text{IPF} = \frac{0.0465\ \text{nm}^3}{0.0741\ \text{nm}^3} = 0.627.$$

EXAMPLE 3.4

Using data from Appendices 1 and 2, calculate the density of MgO.

SOLUTION

From Example 3.3, $a = 0.420$ nm, which gave a unit-cell volume of $0.0741\ \text{nm}^3$. The density of the unit cell is

$$\begin{aligned} \rho &= \frac{[4(24.31\ \text{g}) + 4(16.00\ \text{g})]/(0.6023 \times 10^{24})}{0.0741\ \text{nm}^3} \times \left(\frac{10^7\ \text{nm}}{\text{cm}}\right)^3 \\ &= 3.61\ \text{g/cm}^3. \end{aligned}$$

PRACTICE PROBLEM 3.4

Calculate the IPF of **(a)** CaO, **(b)** FeO, and **(c)** NiO. All of these compounds share the NaCl-type structure. **(d)** Is there a unique IPF value for the NaCl-type structure? Explain. (See Example 3.3.)

PRACTICE PROBLEM 3.5

Calculate the density of CaO. (See Example 3.4.)

3.4 Polymeric Structures

In Chapters 1 and 2, we defined the polymers category of materials by the chain-like structure of long polymeric molecules (e.g., Figure 2.15). Compared with the stacking of individual atoms and ions in metals and ceramics, the arrangement of these long molecules into a regular and repeating pattern is difficult. As a result, most commercial plastics are to a large degree noncrystalline. In those regions of the microstructure that are crystalline, the structure tends to be quite complex. The complexity of the unit cells of common polymers is generally beyond the scope of this text, but one relatively simple example will be shown.

Polyethylene, $+C_2H_4+_n$, is chemically quite simple. However, the relatively elaborate way in which the long-chain molecule folds back and forth on itself is illustrated in Figure 3.19. Figure 3.19(a) shows an orthorhombic unit cell, a common crystal system for polymeric crystals. For metals and ceramics, knowledge of the unit-cell structure implies knowledge of the crystal structure over a large volume. For polymers, we must be more cautious. Single crystals of polyethylene are difficult to grow. When produced (by cooling a dilute solution), they tend to be thin platelets, about 10 nm thick. Since polymer chains are generally several hundred nanometers long, the chains must be folded back and forth in a sort of atomic-scale weaving [as illustrated in Figure 3.19(b)].

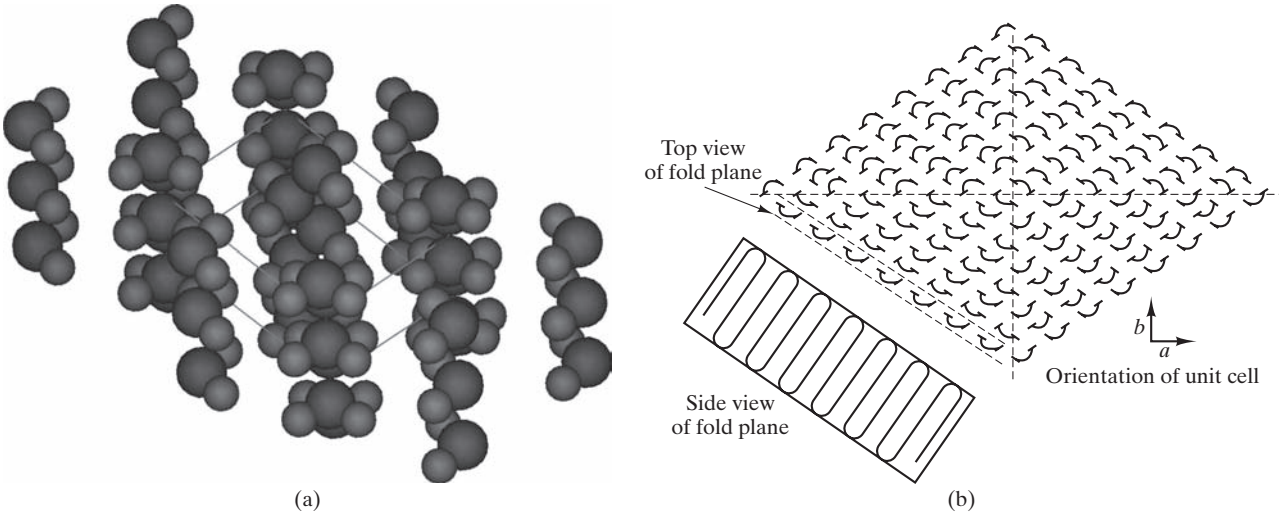

FIGURE 3.19 *(a) Arrangement of polymeric chains in the unit cell of polyethylene. The dark spheres are carbon atoms, and the light spheres are hydrogen atoms. The unit-cell dimensions are* 0.255 *nm* × 0.494 *nm* × 0.741 *nm. (Courtesy of Accelrys, Inc.) (b) Weaving-like pattern of folded polymeric chains that occurs in thin crystal platelets of polyethylene. (From D. J. Williams,* Polymer Science and Engineering*, Prentice-Hall, Inc., Englewood Cliffs, NJ, 1971.)*

EXAMPLE 3.5

Calculate the number of C and H atoms in the polyethylene unit cell [Figure 3.19(a)], given a density of 0.9979 g/cm^3.

SOLUTION

Figure 3.19(a) gives unit-cell dimensions that allow calculation of volume:

$$V = (0.741\ \text{nm})(0.494\ \text{nm})(0.255\ \text{nm}) = 0.0933\ \text{nm}^3.$$

There will be some multiple (n) of C_2H_4 units in the unit cell with atomic mass:

$$m = \frac{n[2(12.01) + 4(1.008)]\ \text{g}}{0.6023 \times 10^{24}} = (4.66 \times 10^{-23}n)\ \text{g}.$$

Therefore, the unit-cell density is

$$\rho = \frac{(4.66 \times 10^{-23}n)\ \text{g}}{0.0933\ \text{nm}^3} \times \left(\frac{10^7\ \text{nm}}{\text{cm}}\right)^3 = 0.9979\ \frac{\text{g}}{\text{cm}^3}.$$

Solving for n gives

$$n = 2.00.$$

As a result, there are

$$4(= 2n)\ \text{C atoms} + 8\ (= 4n)\ \text{H atoms per unit cell.}$$

PRACTICE PROBLEM 3.6

How many unit cells are contained in 1 kg of commercial polyethylene that is 50 vol % crystalline (balance amorphous) and that has an overall product density of 0.940 Mg/m^3? (See Example 3.5.)

3.5 Semiconductor Structures

The technology developed by the semiconductor industry for growing single crystals has led to crystals of phenomenally high degrees of perfection. All crystal structures shown in this chapter imply structural perfection. However, all structures are subject to various imperfections, which will be discussed in Chapter 4. The "perfect" structures described in this section are approached in real materials more closely than in any other category.

A single structure dominates the semiconductor industry. The elemental semiconductors (Si, Ge, and gray Sn) share the **diamond cubic** structure shown in Figure 3.20. This structure is built on an fcc Bravais lattice with two atoms associated with each lattice point and eight atoms per unit cell. A key feature of this structure is that it accommodates the tetrahedral bonding configuration of these group IV A elements.

A small cluster of elements adjacent to group IV A forms semiconducting compounds, which tend to be MX-type compounds with combinations of atoms having an average valence of 4+. For example, GaAs combines the 3+ valence

THE MATERIAL WORLD

Growing a (Nearly) Perfect Crystal

The technological and cultural revolution created by the many products based on the modern integrated circuit begins with single crystals of exceptionally high chemical purity and structural perfection. More than any other commercially produced materials, these crystals represent the ideal described in this chapter. The vast majority of integrated circuits are produced on thin slices (wafers) of **silicon** single crystals [see photo, which shows a state-of-the-art 300 mm (12 in.) diameter wafer]. The systematic procedures for producing fine-scale electrical circuits on these wafers are discussed in some detail in Chapter 13.

As shown in the drawing, a large crystal of silicon is produced by pulling a small "seed" crystal up from a crucible containing molten silicon. The high melting point of silicon (T_m = 1,414°C) calls for a crucible made of high-purity SiO_2 glass. Heat is provided by radio-frequency (RF) inductive heating coils. The seed crystal is inserted into the melt and slowly withdrawn. Crystal growth occurs as the liquid silicon freezes next to the seed crystal, with individual atoms stacking against those in the seed. Successive layers of atomic planes are added at the liquid–solid interface. The overall growth rate is approximately 10 μm/s. The resulting large crystals are sometimes called *ingots* or *boules*. This overall process is generally called the *Czochralski* or *Teal–Little technique*. As noted in Chapter 13, the economics of a circuit fabrication on single crystal wafers drives crystal growers to produce as large a diameter crystal as possible. The industry standard for crystal and corresponding wafer diameters has increased over the years to the current 300 mm.

(Courtesy of SEMATECH.)

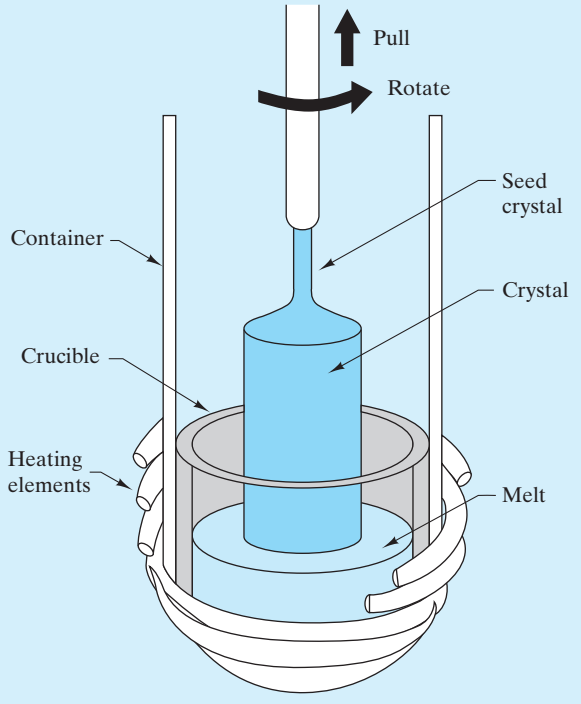

Schematic of growth of single crystals using the Czochralski technique. (From J.W. Mayer and S. S. Lau, Electronic Materials Science: For Integrated Circuits in Si and GaAs, *Macmillan Publishing Company, New York, 1990.)*

The basic science and technology involved in growing single crystals as illustrated here have been joined by considerable "art" in adjusting the various specifics of the crystal-growing apparatus and procedures. The highly specialized process of growing these crystals is largely the focus of companies separate from those that fabricate circuits. The structural perfection provided by the Czochralski technique is joined with the ability to chemically purify the resulting crystal by the zone refining technique, as discussed in the Feature Box for Chapter 9 and in Chapter 13.

of gallium with the 5+ valence of arsenic, and CdS combines the 2+ valence of cadmium with the 6+ valence of sulfur. GaAs and CdS are examples of a **III–V compound** and a **II–VI compound**, respectively. Many of these simple MX compounds crystallize in a structure closely related to the diamond cubic. Figure 3.21 shows the **zinc blende** (ZnS) structure, which is essentially the diamond cubic structure with Zn^{2+} and S^{2-} ions alternating in the atom positions. This is again the fcc Bravais lattice, but with two oppositely charged ions associated with each lattice site rather

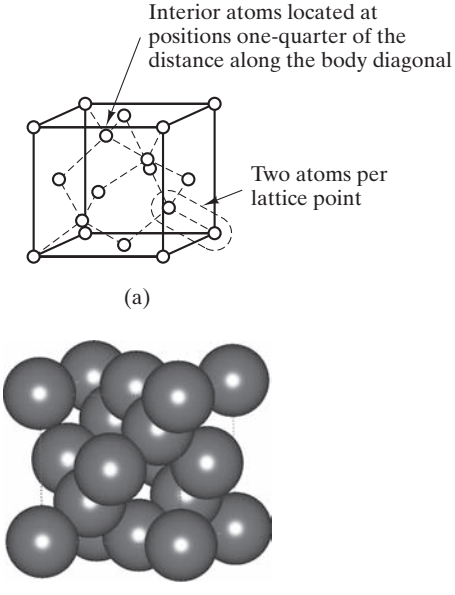

Structure: diamond cubic
Bravais lattice: fcc
Atoms/unit cell: $4 + 6 \times \frac{1}{2} + 8 \times \frac{1}{8} = 8$
Typical semiconductors: Si, Ge, and gray Sn

FIGURE 3.20 *Diamond cubic unit cell showing (a) atom positions. There are two atoms per lattice point (note the outlined example). Each atom is tetrahedrally coordinated. (b) The actual packing of full-size atoms associated with the unit cell. [Part (b) courtesy of Accelrys, Inc.]*

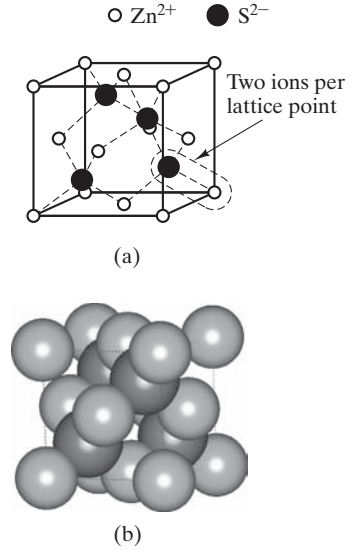

Structure: Zinc blende (ZnS) type
Bravais lattice: fcc
Ions/unit cell: $4Zn^{2+} + 4S^{2-}$
Typical semiconductors:
GaAs, AlP, InSb (III–V compounds),
ZnS, ZnSe, CdS, HgTe (II–VI compounds)

FIGURE 3.21 *Zinc blende (ZnS) unit cell showing (a) ion positions. There are two ions per lattice point (note the outlined example). Compare this structure with the diamond cubic structure [Figure 3.20(a)]. (b) The actual packing of full-size ions associated with the unit cell. [Part (b) courtesy of Accelrys, Inc.]*

than two like atoms. There are eight ions (four Zn^{2+} and four S^{2-}) per unit cell. This structure is shared by both III–V compounds (e.g., GaAs, AlP, and InSb) and II–VI compounds (e.g., ZnSe, CdS, and HgTe).

EXAMPLE 3.6

Calculate the APF for the diamond cubic structure (Figure 3.20).

SOLUTION

Because of the tetrahedral bonding geometry of the diamond cubic structure, the atoms lie along body diagonals. Inspection of Figure 3.20 indicates that this orientation of atoms leads to the equality

$$2r_{Si} = \frac{1}{4}(\text{body diagonal}) = \frac{\sqrt{3}}{4}a$$

or

$$a = \frac{8}{\sqrt{3}}r_{Si}.$$

The unit-cell volume then, is,

$$V_{\text{unit cell}} = a^3 = (4.62)^3 r_{Si}^3 = 98.5 r_{Si}^3.$$

The volume of the eight Si atoms in the unit cell is

$$V_{\text{atoms}} = 8 \times \frac{4}{3}\pi r_{Si}^3 = 33.5 r_{Si}^3,$$

which gives an atomic packing factor of

$$\text{APF} = \frac{33.5 r_{Si}^3}{98.5 r_{Si}^3} = 0.340.$$

Note. This result represents a very open structure compared with the tightly packed metals' structures described in Section 3.2 (e.g., APF = 0.74 for fcc and hcp metals).

EXAMPLE 3.7

Using the data of Appendices 1 and 2, calculate the density of silicon.

SOLUTION

From Example 3.6,

$$V_{\text{unit cell}} = 98.5 r_{Si}^3 = 98.5\ (0.117\ \text{nm})^3$$
$$= 0.158\ \text{nm}^3,$$

giving a density of

$$\rho = \frac{8 \text{ atoms}}{0.158 \text{ nm}^3} \times \frac{28.09 \text{ g}}{0.6023 \times 10^{24} \text{ atoms}} \times \left(\frac{10^7 \text{nm}}{\text{cm}}\right)^3$$
$$= 2.36 \text{ g/cm}^3.$$

As for previous calculations, a slight discrepancy between this result and Appendix 1 data (e.g., $\rho_{Si} = 2.33 \text{ g/cm}^3$) is the result of not having another significant figure with the atomic radius data of Appendix 2.

PRACTICE PROBLEM 3.7

In Example 3.6, we find the atomic packing factor for silicon to be quite low compared with that of the common metal structures. Comment on the relationship between this characteristic and the nature of bonding in semiconductor silicon.

PRACTICE PROBLEM 3.8

Calculate the density of germanium using data from Appendices 1 and 2. (See Example 3.7.)

3.6 Lattice Positions, Directions, and Planes

There are a few basic rules for describing geometry in and around a unit cell. These rules and associated notations are used uniformly by crystallographers, geologists, materials scientists, and others who must deal with crystalline materials. What we are about to learn, then, is a vocabulary that allows us to communicate efficiently about crystalline structure. This vocabulary will prove to be most useful when we begin to deal with structure-sensitive properties later in the book.

Figure 3.22 illustrates the notation for describing **lattice positions** expressed as fractions or multiples of unit-cell dimensions. For example, the body-centered position in the unit cell projects midway along each of the three unit-cell edges and is designated the $\frac{1}{2}\frac{1}{2}\frac{1}{2}$ position. One aspect of the nature of crystalline structure is that a given lattice position in a given unit cell is structurally equivalent to the same position in any other unit cell of the same structure. These equivalent positions are connected by **lattice translations** consisting of integral multiples of lattice constants along directions parallel to crystallographic axes (Figure 3.23).

Figure 3.24 illustrates the notation for describing **lattice directions**. These directions are always expressed as sets of integers, which are obtained by identifying the *smallest integer positions* intercepted by the line from the origin of the crystallographic axes. To distinguish the notation for a direction from that of a position, the direction integers are enclosed in square brackets. The use of square brackets is important and is the standard designation for specific lattice directions. Other symbols are used to designate other geometrical features. Returning

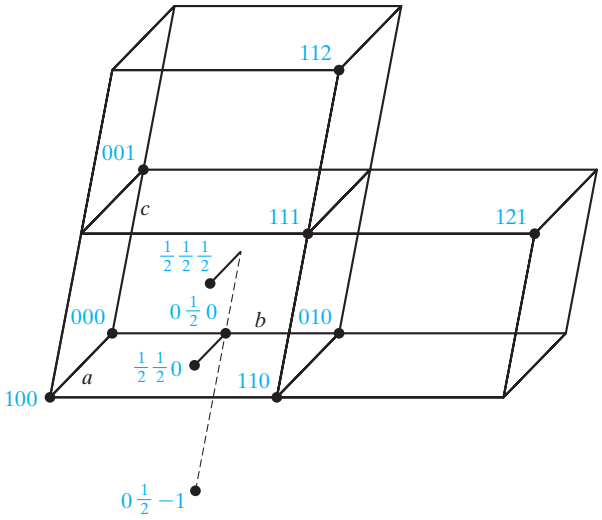

FIGURE 3.22 *Notation for lattice positions.*

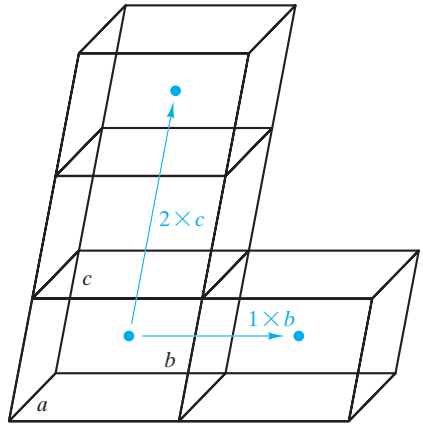

FIGURE 3.23 *Lattice translations connect structurally equivalent positions (e.g., the body center) in various unit cells.*

to Figure 3.24, we note that the line from the origin of the crystallographic axes through the $\frac{1}{2}\frac{1}{2}\frac{1}{2}$ body-centered position can be extended to intercept the 111 unit-cell corner position. Although further extension of the line will lead to interception of other integer sets (e.g., 222 or 333), the 111 set is the smallest. As a result, that direction is referred to as the [111].

When a direction moves along a negative axis, the notation must indicate this movement. For example, the bar above the final integer in the $[11\bar{1}]$ direction in Figure 3.24 designates that the line from the origin has penetrated the 11–1 position. Note that the directions [111] and $[11\bar{1}]$ are structurally very similar. Both are body diagonals through identical unit cells. In fact, if you look at all body diagonals associated with the cubic crystal system, it is apparent that they are structurally identical, differing only in their orientation in space (Figure 3.25). In other words, the $[11\bar{1}]$ direction would become the [111] direction if we made a different choice of crystallographic axes orientations. Such a set of directions, which are structurally equivalent, is called a **family of directions** and is designated by angular brackets, $\langle\ \rangle$. An example of body diagonals in the cubic system is

$$\langle 111 \rangle = [\bar{1}11], [1\bar{1}1], [11\bar{1}], [\bar{1}\bar{1}\bar{1}], [1\bar{1}\bar{1}], [\bar{1}1\bar{1}], [\bar{1}\bar{1}1]. \qquad \textbf{(3.1)}$$

In future chapters, especially when dealing with calculations of mechanical properties, it will be useful to know the angle between directions. In general, the angles between directions can be determined by careful visualization and trigonometric calculation. In the frequently encountered cubic system, the angle can be determined from the relatively simple calculation of a dot product of two vectors. Taking directions $[uvw]$ and $[u'v'w']$ as vectors $\mathbf{D} = u\mathbf{a} + v\mathbf{b} + w\mathbf{c}$ and $\mathbf{D}' = u'\mathbf{a} + v'\mathbf{b} + w'\mathbf{c}$, you can determine the angle, δ, between these two directions by

$$\mathbf{D} \cdot \mathbf{D}' = |\mathbf{D}||\mathbf{D}'|\cos\delta \qquad \textbf{(3.2)}$$

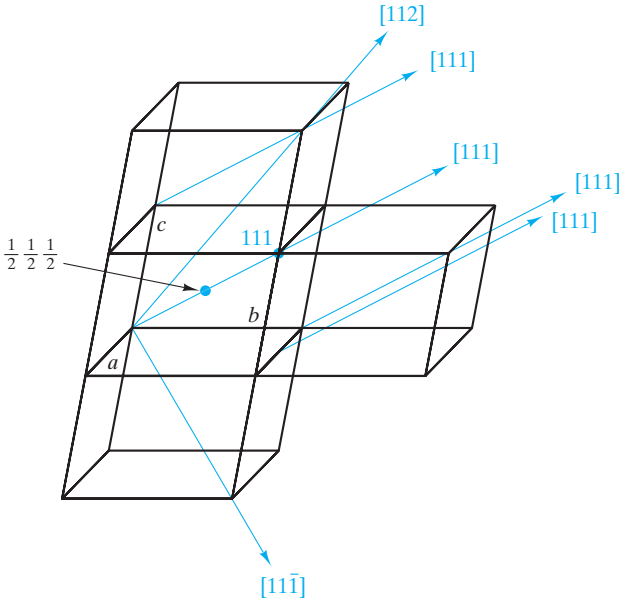

FIGURE 3.24 *Notation for lattice directions. Note that parallel [uvw] directions (e.g.,* [111]*) share the same notation because only the origin is shifted.*

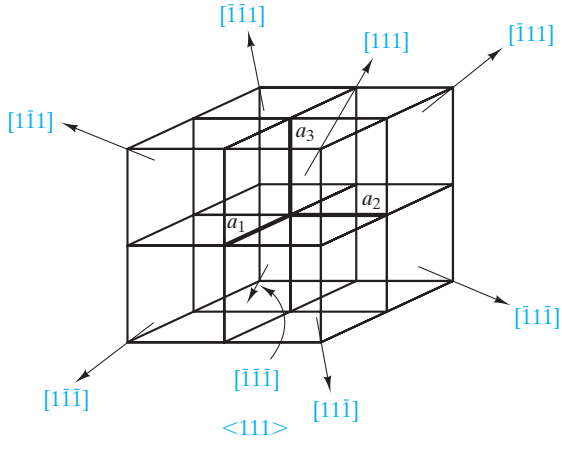

FIGURE 3.25 *Family of directions,* ⟨111⟩*, representing all body diagonals for adjacent unit cells in the cubic system.*

$$\cos\delta = \frac{\mathbf{D}\cdot\mathbf{D}'}{|\mathbf{D}||\mathbf{D}'|} = \frac{uu' + vv' + ww'}{\sqrt{u^2 + v^2 + w^2}\sqrt{(u')^2 + (v')^2 + (w')^2}}. \tag{3.3}$$

It is important to remember that Equations 3.2 and 3.3 apply to the cubic system only.

Another quantity of interest in future calculations is the **linear density** of atoms along a given direction. Again, a general approach to such a calculation is careful visualization and trigonometric calculation. A streamlined approach in the case where atoms are uniformly spaced along a given direction is to determine the repeat distance, r, between adjacent atoms. The linear density is simply the inverse, r^{-1}. In making linear-density calculations for the first time, it is important to keep in mind that we are counting only those atoms whose centers lie directly on the direction line and not any that might intersect that line off-center.

Figure 3.26 illustrates the notation for describing **lattice planes**, which are planes in a crystallographic lattice. As for directions, these planes are expressed as a set of integers, known as **Miller* indices**. Obtaining these integers is a more elaborate process than was required for directions. The integers represent the inverse of axial intercepts. For example, consider the plane (210) in Figure 3.26a. As with the square brackets of direction notation, the parentheses serve as standard notation for planes. The (210) plane intercepts the a-axis at $\frac{1}{2}a$ and the b-axis

*William Hallowes Miller (1801–1880), British crystallographer, was a major contributor along with Bravais to 19th-century crystallography. His efficient system of labeling crystallographic planes was but one of many achievements.

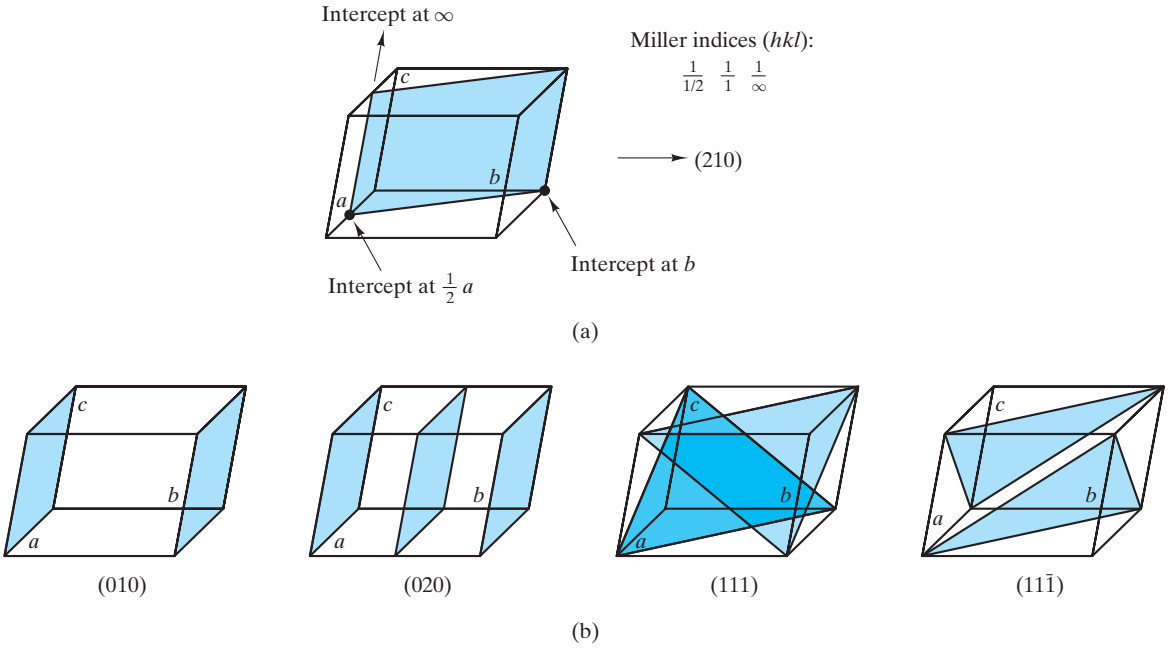

FIGURE 3.26 *Notation for lattice planes. (a) The* (210) *plane illustrates Miller indices (hkl). (b) Additional examples.*

at *b,* and it is parallel to the *c*-axis (in effect, intercepting it at ∞). The inverses of the axial intercepts are $1/\frac{1}{2}$, 1/1, and $1/\infty$, respectively. These inverse intercepts give the 2, 1, and 0 integers leading to the (210) notation. At first, the use of these Miller indices seems like extra work. In fact, however, they provide an efficient labeling system for crystal planes and play an important role in equations dealing with diffraction measurements (Section 3.7). The general notation for Miller indices is (*hkl*), and it can be used for any of the seven crystal systems. Because the hexagonal system can be conveniently represented by four axes, a four-digit set of **Miller–Bravais indices** (*hkil*) can be defined as shown in Figure 3.27. Since only three axes are necessary to define the three-dimensional geometry of a crystal, one of the integers in the Miller–Bravais system is redundant. Once a plane intersects any two axes in the basal plane at the bottom of the unit cell (which contains axes a_1, a_2, and a_3 in Figure 3.27), the intersection with the third basal plane axis is determined. As a result, it can be shown that $h + k = -i$ for any plane in the hexagonal system, which also permits any such hexagonal system plane to be designated by Miller–Bravais indices (*hkil*) or by Miller indices (*hkl*). For the plane shown in Figure 3.27, the designation can be $(01\bar{1}0)$ or (010).

As for structurally equivalent directions, we can group structurally equivalent planes as a **family of planes** with Miller or Miller–Bravais indices enclosed in braces, {*hkl*} or {*hkil*}. Figure 3.28 illustrates that the faces of a unit cell in the cubic system are of the {100} family with

$$\{100\} = (100), (010), (001), (\bar{1}00), (0\bar{1}0), (00\bar{1}). \tag{3.4}$$

Future chapters will require calculation of **planar densities** of atoms (number per unit area) analogous to the linear densities mentioned before. As with linear densities, only those atoms centered on the plane of interest are counted.

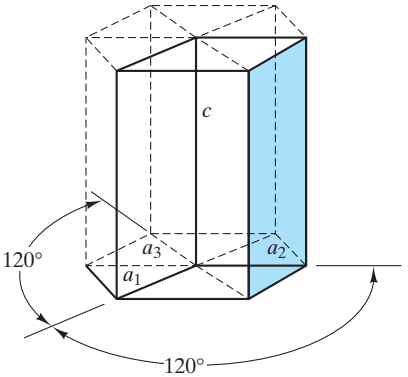

Miller–Bravais indices (*hkil*): $\frac{1}{\infty}, \frac{1}{1}, \frac{1}{-1}, \frac{1}{\infty} \rightarrow (01\bar{1}0)$
Note: $h + k = -i$

FIGURE 3.27 *Miller–Bravais indices (hkil) for the hexagonal system.*

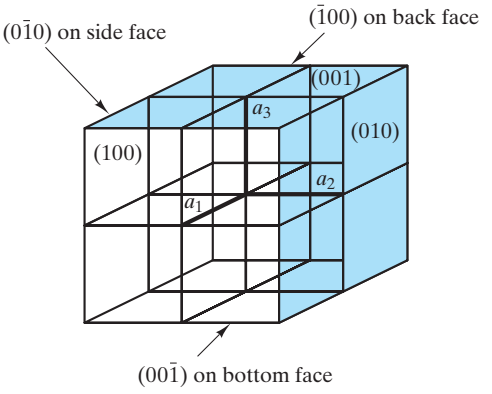

{100}

FIGURE 3.28 *Family of planes,* {100}*, representing all faces of unit cells in the cubic system.*

EXAMPLE 3.8

Using Table 3.2, list the face-centered lattice-point positions for **(a)** the fcc Bravais lattice and **(b)** the *face-centered orthorhombic* (fco) lattice.

SOLUTION

(a) For the face-centered positions, $\frac{1}{2}\frac{1}{2}0, \frac{1}{2}0\frac{1}{2}, 0\frac{1}{2}\frac{1}{2}1, \frac{1}{2}1\frac{1}{2}, 1\frac{1}{2}\frac{1}{2}$.

(b) Same answer as part (a). Lattice parameters do not appear in the notation for lattice positions.

EXAMPLE 3.9

Which lattice points lie on the [110] direction in the fcc and fco unit cells of Table 3.2?

SOLUTION

Sketching this case gives

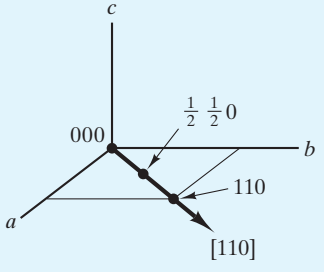

The lattice points are 000, $\frac{1}{2}\frac{1}{2}0$, and 110 for either system, fcc or fco.

EXAMPLE 3.10

List the members of the $\langle 110 \rangle$ family of directions in the cubic system.

SOLUTION

The family of directions constitutes all face diagonals of the unit cell, with two such diagonals on each face for a total of 12 members:

$$\langle 110 \rangle = [110], [1\bar{1}0], [\bar{1}10], [\bar{1}\bar{1}0], [101], [10\bar{1}], [\bar{1}01],$$
$$[\bar{1}0\bar{1}], [011], [01\bar{1}], [0\bar{1}1], [0\bar{1}\bar{1}].$$

EXAMPLE 3.11

What is the angle between the [110] and [111] directions in the cubic system?

SOLUTION

From Equation 3.3,

$$\delta = \arccos \frac{uu' + vv' + ww'}{\sqrt{u^2 + v^2 + w^2}\sqrt{(u')^2 + (v')^2 + (w')^2}}$$
$$= \arccos \frac{1 + 1 + 0}{\sqrt{2}\sqrt{3}}$$
$$= \arccos 0.816$$
$$= 35.3°.$$

EXAMPLE 3.12

Identify the axial intercepts for the $(3\bar{1}1)$ plane.

SOLUTION

For the a axis, intercept $= \frac{1}{3}a$; for the b axis, intercept $= \frac{1}{-1}b = -b$; and for the c axis, intercept $= \frac{1}{1}c = c$.

EXAMPLE 3.13

List the members of the {110} family of planes in the cubic system.

SOLUTION

$$\{110\} = (110), (1\bar{1}0), (\bar{1}10), (\bar{1}\bar{1}0), (101), 10\bar{1}), (\bar{1}01),$$
$$(\bar{1}0\bar{1}), (011), (01\bar{1}), (0\bar{1}1), (0\bar{1}\bar{1}).$$

(Compare this answer with that for Example 3.10.)

EXAMPLE 3.14

Calculate the linear density of atoms along the [111] direction in **(a)** bcc tungsten and **(b)** fcc aluminum.

SOLUTION

(a) For a bcc structure (Figure 3.4), atoms touch along the [111] direction (a body diagonal). Therefore, the repeat distance is equal to one atomic diameter. Taking data from Appendix 2, we find that the repeat distance is

$$\begin{aligned} r &= d_{\text{W atom}} = 2r_{\text{W atom}} \\ &= 2(0.137\ \text{nm}) = 0.274\ \text{nm}. \end{aligned}$$

Therefore,

$$r^{-1} = \frac{1}{0.274\ \text{nm}} = 3.65\ \text{atoms/nm}.$$

(b) For an fcc structure, only one atom is intercepted along the body diagonal of a unit cell. To determine the length of the body diagonal, we can note that two atomic diameters equal the length of a face diagonal (see Figure 3.5). Using data from Appendix 2, we have

$$\begin{aligned} \text{face diagonal length} &= 2d_{\text{Al atom}} \\ &= 4r_{\text{Al atom}} = \sqrt{2}a \end{aligned}$$

or the lattice parameter is

$$\begin{aligned} a &= \frac{4}{\sqrt{2}} r_{\text{Al atom}} \quad \text{(see also Table 3.3)} \\ &= \frac{4}{\sqrt{2}}(0.143\ \text{nm}) = 0.404\ \text{nm}. \end{aligned}$$

The repeat distance is

$$\begin{aligned} r &= \text{body diagonal length} = \sqrt{3}a \\ &= \sqrt{3}(0.404\ \text{nm}) \\ &= 0.701\ \text{nm}, \end{aligned}$$

which gives a linear density of

$$r^{-1} = \frac{1}{0.701\ \text{nm}} = 1.43\ \text{atoms/nm}.$$

EXAMPLE 3.15

Calculate the planar density of atoms in the (111) plane of **(a)** bcc tungsten and **(b)** fcc aluminum.

SOLUTION

(a) For the bcc structure (Figure 3.4), the (111) plane intersects only corner atoms in the unit cell:

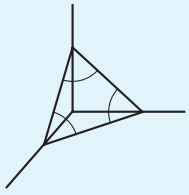

Following the calculations of Example 3.14a, we have

$$\sqrt{3}a = 4r_{\text{W atom}}$$

or

$$a = \frac{4}{\sqrt{3}} r_{\text{W atom}} = \frac{4}{\sqrt{3}}(0.137\ \text{nm}) = 0.316\ \text{nm}.$$

Face diagonal length, l, is then

$$l = \sqrt{2}a = \sqrt{2}(0.316\ \text{nm}) = 0.447\ \text{nm}.$$

The area of the (111) plane within the unit cell is

$$A = \frac{1}{2}bh = \frac{1}{2}(0.447\ \text{nm})\left(\frac{\sqrt{3}}{2} \times 0.447\ \text{nm}\right)$$

$$= 0.0867\ \text{nm}^2.$$

There is $\frac{1}{6}$ atom (i.e., $\frac{1}{6}$ of the circumference of a circle) at each corner of the equilateral triangle formed by the (111) plane in the unit cell. Therefore,

$$\text{atomic density} = \frac{3 \times \frac{1}{6}\ \text{atom}}{A}$$

$$= \frac{0.5\ \text{atom}}{0.0867\ \text{nm}^2} = 5.77 \frac{\text{atoms}}{\text{nm}^2}.$$

(b) For the fcc structure (Figure 3.5), the (111) plane intersects three corner atoms plus three face-centered atoms in the unit cell:

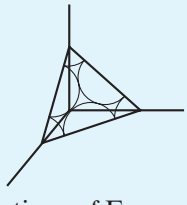

Following the calculations of Example 3.14(b), we obtain the face diagonal length

$$l = \sqrt{2}a = \sqrt{2}(0.404\text{ nm}) = 0.572\text{ nm}.$$

The area of the (111) plane within the unit cell is

$$A = \frac{1}{2}bh = \frac{1}{2}(0.572\text{ nm})\left(\frac{\sqrt{3}}{2}0.572\text{ nm}\right)$$
$$= 0.142\text{ nm}^2.$$

There are $3 \times \frac{1}{6}$ corner atoms plus $3 \times \frac{1}{2}$ face-centered atoms within this area, giving

$$\text{atomic density} = \frac{3 \times \frac{1}{6} + 3 \times \frac{1}{2}\text{ atoms}}{0.142\text{ nm}^2} = \frac{2\text{ atoms}}{0.142\text{ nm}^2}$$
$$= 14.1\text{ atoms/nm}^2.$$

EXAMPLE 3.16

Calculate the linear density of ions in the [111] direction of MgO.

SOLUTION

Figure 3.9 shows that the body diagonal of the unit cell intersects one Mg^{2+} and one O^{2-}. Following the calculations of Example 3.3, we find that the length of the body diagonal is

$$l = \sqrt{3}a = \sqrt{3}(0.420\text{ nm}) = 0.727\text{ nm}.$$

The ionic linear densities, then, are

$$\frac{1\text{ Mg}^{2+}}{0.727\text{ nm}} = 1.37\text{ Mg}^{2+}/\text{nm}$$

and, similarly,

$$1.37\text{ O}^{2-}/\text{nm},$$

giving

$$(1.37\text{ Mg}^{2+} + 1.37\text{ O}^{2-})/\text{nm}.$$

EXAMPLE 3.17

Calculate the planar density of ions in the (111) plane of MgO.

SOLUTION

There are really two separate answers to this problem. Using the unit cell of Figure 3.9, we see an arrangement comparable to an fcc metal:

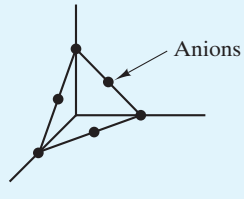

However, we could similarly define a unit cell with its origin on a cation site (rather than on an anion site as shown in Figure 3.9). In this case, the (111) plane would have a comparable arrangement of cations:

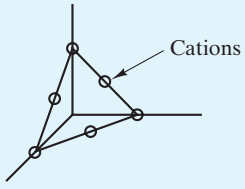

In either case, there are two ions per (111) "triangle." From Example 3.3, we know that $a = 0.420$ nm. The length of each (111) triangle side (i.e., a unit-cell face diagonal) is

$$l = \sqrt{2}a = \sqrt{2}(0.420 \text{ nm}) = 0.594 \text{ nm}.$$

The planar area, then, is

$$A = \frac{1}{2}bh = \frac{1}{2}(0.594 \text{ nm})\left(\frac{\sqrt{3}}{2}0.594 \text{ nm}\right) = 0.153 \text{ nm}^2,$$

which gives

$$\text{ionic density} = \frac{2 \text{ ions}}{0.153 \text{ nm}^2} = 13.1 \text{ nm}^{-2}$$

or

$$13.1(\text{Mg}^{2+} \textit{ or } \text{O}^{2-})/\text{nm}^2.$$

EXAMPLE 3.18

Calculate the linear density of atoms along the [111] direction in silicon.

SOLUTION

We must use some caution in this problem. Inspection of Figure 3.20 indicates that atoms along the [111] direction (a body diagonal) are not uniformly spaced. Therefore, the r^{-1} calculations of Example 3.14 are not appropriate.

Referring to the comments of Example 3.6, we can see that two atoms are centered along a given body diagonal (e.g., $\frac{1}{2}$ atom at 000, 1 atom at $\frac{1}{4}\frac{1}{4}\frac{1}{4}$, and $\frac{1}{2}$ atom at 111). If we take the body diagonal length in a unit cell as *l*,

$$2r_{Si} = \frac{1}{4}l$$

or

$$l = 8r_{Si}.$$

From Appendix 2,

$$l = 8(0.117 \text{ nm}) = 0.936 \text{ nm}.$$

Therefore, the linear density is

$$\text{linear density} = \frac{2 \text{ atoms}}{0.936 \text{ nm}} = 2.14 \frac{\text{atoms}}{\text{nm}}.$$

EXAMPLE 3.19

Calculate the planar density of atoms in the (111) plane of silicon.

SOLUTION

Close observation of Figure 3.20 shows that the four interior atoms in the diamond cubic structure do not lie on the (111) plane. The result is that the atom arrangement in this plane is precisely that for the metallic fcc structure [see Example 3.15(b)]. Of course, the atoms along [110]-type directions in the diamond cubic structure do not touch as in fcc metals.

As calculated in Example 3.15(b), there are two atoms in the equilateral triangle bounded by sides of length $\sqrt{2}a$. From Example 3.6 and Appendix 2, we see that

$$a = \frac{8}{\sqrt{3}}(0.117 \text{ nm}) = 0.540 \text{ nm}$$

and

$$\sqrt{2}a = 0.764 \text{ nm},$$

giving a triangle area of

$$A = \frac{1}{2}bh = \frac{1}{2}(0.764 \text{ nm})\left(\frac{\sqrt{3}}{2}0.764 \text{ nm}\right)$$
$$= 0.253 \text{ nm}^2$$

and a planar density of

$$\frac{2 \text{ atoms}}{0.253 \text{ nm}^2} = 7.91 \frac{\text{atoms}}{\text{nm}^2}.$$

PRACTICE PROBLEM 3.18

Calculate the linear density of ions along the [111] direction for CaO. (See Example 3.16.)

PRACTICE PROBLEM 3.19

Calculate the planar density of ions in the (111) plane for CaO. (See Example 3.17.)

PRACTICE PROBLEM 3.20

Find the linear density of atoms along the [111] direction for germanium. (See Example 3.18.)

PRACTICE PROBLEM 3.21

Find the planar density of atoms in the (111) plane for germanium. (See Example 3.19.)

3.7 X-Ray Diffraction

This chapter has introduced a large variety of crystal structures. We now end with a brief description of **x-ray diffraction**, a powerful experimental tool.

There are many ways in which x-ray diffraction is used to measure the crystal structure of engineering materials. It can be used to determine the structure of a new material, or the known structure of a common material can be used as a source of chemical identification.

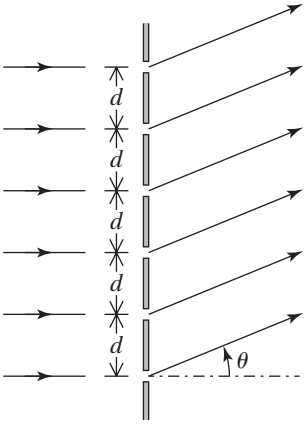

FIGURE 3.29 *Diffraction grating for visible light. Evenly spaced slits in the plate serve as light-scattering centers. (From H.D. Young and R.A. Freedman,* University Physics, *11th ed., Pearson/Addison Wesley, New York, 2004.)*

Diffraction is the result of radiation being scattered by a regular array of scattering centers whose spacing is about the same as the wavelength of the radiation. For example, regularly spaced, parallel slits about 1 μm apart cause diffraction of visible light (electromagnetic radiation with a wavelength just under 1 μm). This *diffraction grating* causes the light to be scattered with a strong intensity in a few specific directions (Figure 3.29). The precise direction of observed scattering is a function of the exact spacing between the slits in the diffraction grating, relative to the wavelength of the incident light. Evenly spaced, parallel scratches on a plate of glass exhibit the same effect. Appendix 2 shows that atoms and ions are on the order of 0.1 nm in size, so we can think of crystal structures as being diffraction gratings on a subnanometer scale. As shown in Figure 3.30, the portion of the electromagnetic spectrum with a wavelength in this range is **x-radiation** (compared to the 1,000-nm range for the wavelength of visible light). As a result, x-ray diffraction is capable of characterizing crystalline structure.

For x-rays, atoms are the scattering centers. The specific mechanism of scattering is the interaction of a photon of electromagnetic radiation with an orbital electron in the atom. A crystal acts as a three-dimensional diffraction grating. Repeated stacking of crystal planes serves the same function as the parallel slits in Figure 3.29. For a simple crystal lattice, the condition for diffraction is shown in Figure 3.31. For diffraction to occur, x-ray beams scattered off adjacent crystal planes must be in phase. Otherwise, destructive interference of waves occurs and

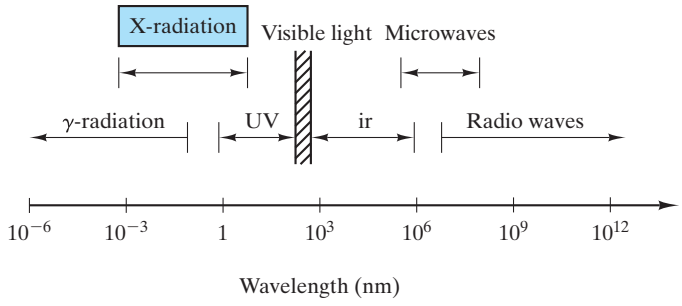

FIGURE 3.30 *Electromagnetic radiation spectrum. X-radiation represents that portion with wavelengths around 0.1 nm.*

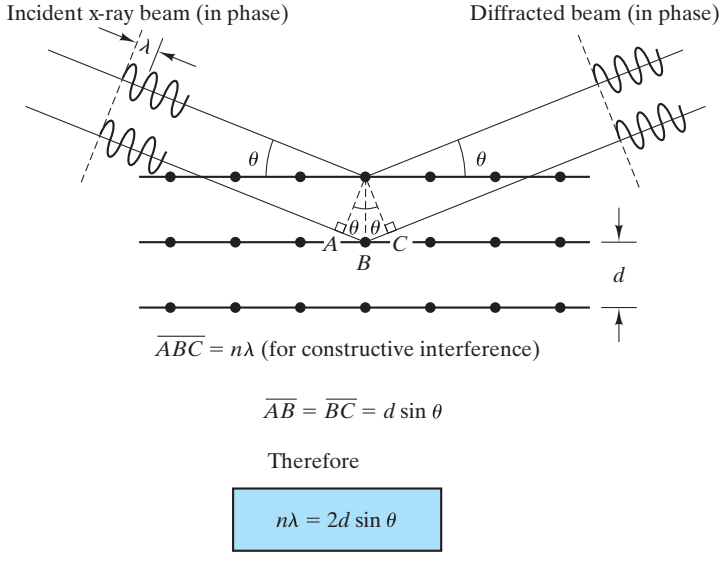

FIGURE 3.31 *Geometry for diffraction of x-radiation. The crystal structure is a three-dimensional diffraction grating. Bragg's law* ($n\lambda = 2d\sin\theta$) *describes the diffraction condition.*

essentially no scattering intensity is observed. At the precise geometry for constructive interference (scattered waves in phase), the difference in path length between the adjacent x-ray beams is some integral number (n) of radiation wavelengths (λ). The relationship that demonstrates this condition is the **Bragg**[†] **equation**

$$n\lambda = 2d\sin\theta, \tag{3.5}$$

where d is the spacing between adjacent crystal planes and θ is the angle of scattering as defined in Figure 3.31. The angle θ is usually referred to as the **Bragg angle**, and the angle 2θ is referred to as the **diffraction angle** because it is the angle measured experimentally (Figure 3.32).

[†]William Henry Bragg (1862–1942) and William Lawrence Bragg (1890–1971), English physicists, were a gifted father-and-son team. They were the first to demonstrate the power of Equation 3.5 by using x-ray diffraction to determine the crystal structures of several alkali halides, such as NaCl. Since this achievement in 1912, the crystal structures of more than 700,000 materials have been catalogued (see the footnote on p. 96).

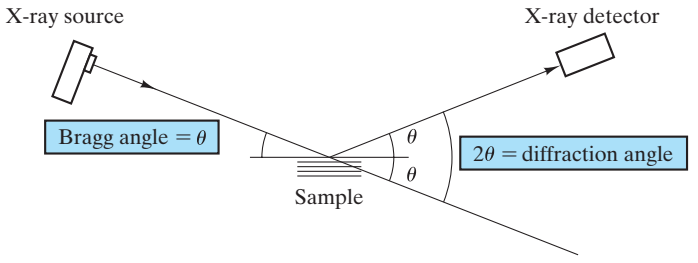

FIGURE 3.32 *Relationship of the Bragg* angle *(θ) and the experimentally measured diffraction* angle *(2θ).*

The magnitude of **interplanar spacing** (d in Equation 3.5) is a direct function of the Miller indices for the plane. For a cubic system, the relationship is fairly simple. The spacing between adjacent hkl planes is

$$d_{hkl} = \frac{a}{\sqrt{h^2 + k^2 + l^2}}, \tag{3.6}$$

where a is the lattice parameter (edge length of the unit cell). For more complex unit-cell shapes, the relationship is more complex. For a *hexagonal system,*

$$d_{hkl} = \frac{a}{\sqrt{\frac{4}{3}(h^2 + hk + k^2) + l^2(a^2/c^2)}}, \tag{3.7}$$

where a and c are the lattice parameters.

Bragg's law (Equation 3.5) is a necessary but insufficient condition for diffraction. It defines the diffraction condition for **primitive unit cells**; that is, those Bravais lattices with lattice points only at unit-cell corners, such as simple cubic and simple tetragonal. Crystal structures with **nonprimitive unit cells** have atoms at additional lattice sites located along a unit-cell edge, within a unit-cell face, or in the interior of the unit cell. The extra scattering centers can cause out-of-phase scattering to occur at certain Bragg angles. The result is that some of the diffraction predicted by Equation 3.5 does not occur. An example of this effect is given in Table 3.4, which gives the **reflection rules** for the common metal structures. These rules show which sets of Miller indices do not produce diffraction as predicted by Bragg's law. Keep in mind that *reflection* here is a casual term in that diffraction rather than true reflection is being described.

TABLE 3.4

Reflection Rules of X-Ray Diffraction for the Common Metal Structures

Crystal structure	Diffraction does not occur when	Diffraction occurs when
Body-centered cubic (bcc)	$h + k + l =$ odd number	$h + k + l =$ even number
Face-centered cubic (fcc)	h, k, l mixed (i.e., both even and odd numbers)	h, k, l unmixed (i.e., are all even numbers or all are odd numbers)
Hexagonal close packed (hcp)	$(h + 2k) = 3n, l$ odd (n is an integer)	All other cases

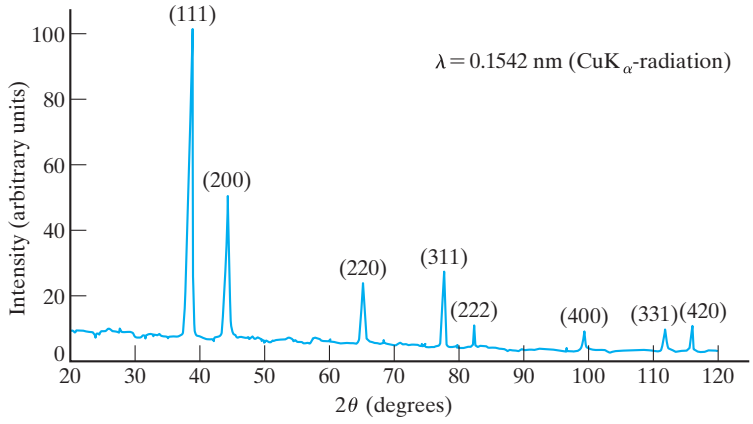

FIGURE 3.33 *Diffraction pattern of aluminum powder. Each peak (in the plot of x-ray intensity versus diffraction angle, 2θ) represents diffraction of the x-ray beam by a set of parallel crystal planes (hkl) in various powder particles.*

POWERS OF 10

Note how small differences in the atomic scale dimensions of crystal structures (interplanar spacings) lead to large angular differences in the x-ray diffraction pattern.

A diffraction pattern for a specimen of aluminum powder is shown in Figure 3.33. Each peak represents a solution to Bragg's law. Because the powder consists of many small crystal grains oriented randomly, a single wavelength of radiation is used to keep the number of diffraction peaks in the pattern to a small, workable number. The experiment is done in a **diffractometer** (Figure 3.34), an electromechanical scanning system. The diffracted beam intensity is monitored electronically by a mechanically driven scanning radiation detector. *Powder patterns* such as those shown in Figure 3.33 are routinely used by materials engineers for comparison against a large collection of known diffraction patterns.* The comparison of an experimental diffraction pattern such as that shown in Figure 3.33 with the database of known diffraction patterns can be done in a few seconds with "search/match" computer software, an integral part of modern diffractometers such as that shown in Figure 3.34. The unique relationship between such patterns and crystal structures provides a powerful tool for chemical identification of powders and polycrystalline materials.

Standard procedure for analyzing the diffraction patterns of powder samples or polycrystalline solids involves the use of $n = 1$ in Equation 3.5. This use is justified in that the nth-order diffraction of any (hkl) plane occurs at an angle identical to the first-order diffraction of the $(nh\ nk\ nl)$ plane [which is, by the way, parallel to (hkl)]. As a result, we can use an even simpler version of Bragg's law for powder diffraction:

$$\lambda = 2d \sin\theta. \tag{3.8}$$

**Powder Diffraction File,* more than 700,000 powder diffraction patterns catalogued by the International Centre for Diffraction Data (ICDD), Newtown Square, PA.

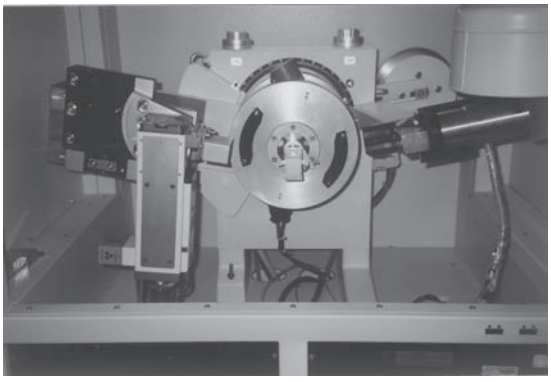

(a)

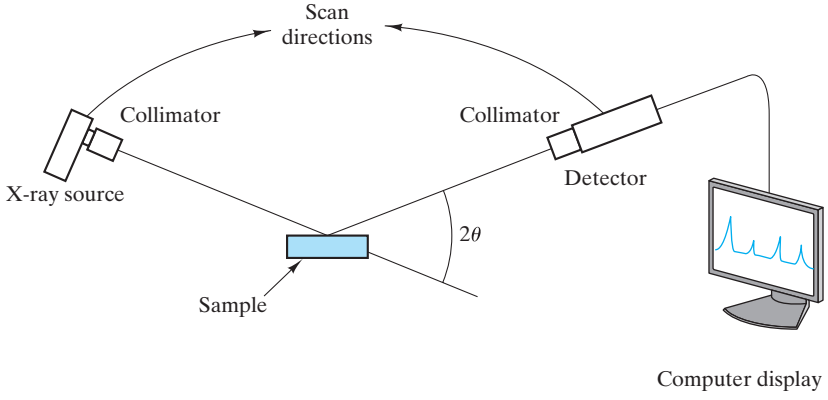

(b)

FIGURE 3.34 *(a) An x-ray diffractometer. (Courtesy of Scintag, Inc.) (b) A schematic of the experiment.*

EXAMPLE 3.20

Using Bragg's law, calculate the diffraction angles (2θ) for the first three peaks in the aluminum powder pattern of Figure 3.33.

SOLUTION

Figure 3.33 indicates that the first three (i.e., lowest-angle) peaks are for (111), (200), and (220). From Example 3.14(b), we note that $a = 0.404$ nm. Therefore, Equation 3.6 yields

$$d_{111} = \frac{0.404 \text{ nm}}{\sqrt{1 + 1 + 1}} = \frac{0.404 \text{ nm}}{\sqrt{3}} = 0.234 \text{ nm},$$

$$d_{200} = \frac{0.404 \text{ nm}}{\sqrt{2^2 + 0 + 0}} = \frac{0.404 \text{ nm}}{2} = 0.202 \text{ nm, and}$$

$$d_{220} = \frac{0.404 \text{ nm}}{\sqrt{2^2 + 2^2 + 0}} = \frac{0.404 \text{ nm}}{\sqrt{8}} = 0.143 \text{ nm}.$$

Noting that $\lambda = 0.1542$ nm in Figure 3.33, Equation 3.8 gives

$$\theta = \arcsin\frac{\lambda}{2d}$$

or

$$\theta_{111} = \arcsin\frac{0.1542 \text{ nm}}{2 \times 0.234 \text{ nm}} = 19.2°$$

or

$$(2\theta)_{111} = 38.5°,$$

$$\theta_{200} = \arcsin\frac{0.1542 \text{ nm}}{2 \times 0.202 \text{ nm}} = 22.4°$$

or

$$(2\theta)_{200} = 44.9°, \text{ and}$$

$$\theta_{220} = \arcsin\frac{0.1542 \text{ nm}}{2 \times 0.143 \text{ nm}} = 32.6°$$

or

$$(2\theta)_{220} = 65.3°.$$

PRACTICE PROBLEM 3.22

The diffraction angles for the first three peaks in Figure 3.33 are calculated in Example 3.20. Calculate the diffraction angles for the remainder of the peaks in Figure 3.33.

Summary

Most materials used by engineers are crystalline in nature; that is, their atomic-scale structure is regular and repeating. This regularity allows the structure to be defined in terms of a fundamental structural unit, the unit cell. There are seven crystal systems, which correspond to the possible unit-cell shapes. Based on these crystal systems, there are 14 Bravais lattices that represent the possible arrangements of points through three-dimensional space. These lattices are the "skeletons" on which the large number of crystalline atomic structures is based.

There are three primary crystal structures observed for common metals: the body-centered cubic (bcc), the face-centered cubic (fcc), and the hexagonal close packed (hcp). These are relatively simple structures, with the fcc and hcp forms representing optimum efficiency in packing equal-sized spheres (i.e., metal atoms). The fcc and hcp structures differ only in the pattern of stacking of close-packed atomic planes.

Chemically more complex than metals, ceramic compounds exhibit a wide variety of crystalline structures. Some, such as the NaCl structure, are similar to the simpler metal structures sharing a common Bravais lattice, but with more than one ion associated with each lattice point. Silica, SiO_2, and the silicates exhibit a wide array of relatively complex arrangements of silica tetrahedra (SiO_4^{4-}). In this chapter, several representative ceramic structures are displayed. Carbon structures are especially interesting in that the well-known graphite and diamond structures have been joined in recent years by the fullerene structures (e.g., buckyballs and buckytubes or carbon nanotubes) and graphene (isolated, single atomic layers of graphite).

Polymers are characterized by long-chain polymeric structures. The elaborate way in which these chains must be folded to form a repetitive pattern produces two effects: (1) The resulting crystal structures are relatively complex and (2) most commercial

polymers are only partially crystalline. The unit-cell structure of polyethylene is illustrated in this chapter.

High-quality single crystals are an important part of *semiconductor* technology, which is possible largely because most semiconductors can be produced in a few relatively simple crystal structures. Elemental semiconductors, such as silicon, have the diamond cubic structure, a modification of the fcc Bravais lattice with two atoms associated with each lattice point. Many compound semiconductors are found in the closely related zinc blende (ZnS) structure, in which the diamond cubic atom positions are retained but with Zn^{2+} and S^{2-} ions alternating on those sites.

There are standard methods for describing the geometry of crystalline structures. These methods give an efficient and systematic notation for lattice positions, directions, and planes.

X-ray diffraction is the standard experimental tool for analyzing crystal structures. The regular atomic arrangement of crystals serves as a subnanometer diffraction grating for *x-radiation* (with a subnanometer wavelength). The use of Bragg's law in conjunction with the reflection rules permits a precise measurement of interplanar spacings in the crystal structure. Polycrystalline (or powdered) materials are routinely analyzed in this way.

Key Terms

General
atomic packing factor (APF) (63)
Bravais lattice (60)
crystal system (60)
family of directions (82)
family of planes (84)
ionic packing factor (67)
lattice constant (60)
lattice direction (81)
lattice parameter (60)
lattice plane (83)
lattice point (60)
lattice position (81)
lattice translation (81)
linear density (83)
Miller–Bravais indices (84)
Miller indices (83)
planar density (88)
point lattice (60)
III–V compounds (79)
II–VI compounds (79)
unit cell (60)

Structures
body-centered cubic (63)
buckminsterfullerene (73)
buckyball (73)
buckytube (73)
carbon nanotube (74)
cesium chloride (67)
corundum (71)
cristobalite (69)
cubic close packed (63)
diamond cubic (77)
face-centered cubic (63)
fluorite (69)
fullerene (73)
graphene (74)
hexagonal close packed (64)
kaolinite (71)
polyethylene (76)
silica (69)
silicon (78)
sodium chloride (67)
zinc blende (79)

Diffraction
Bragg angle (94)
Bragg equation (94)
Bragg's law (95)
diffraction (93)
diffraction angle (94)
diffractometer (96)
interplanar spacing (95)
nonprimitive unit cells (95)
primitive unit cells (95)
reflection rules (95)
x-radiation (93)
x-ray diffraction (93)

References

Accelrys, Inc., San Diego, CA. Computer-generated crystal structures of a wide range of materials are available using software originally developed for product development in the biological sciences.

Barrett, C. S., and **T. B. Massalski,** *Structure of Metals,* 3rd revised ed., Pergamon Press, New York, 1980. This text includes substantial coverage of x-ray diffraction techniques.

Billmeyer, F. W., *Textbook of Polymer Science,* 3rd ed., John Wiley & Sons, Inc., New York, 1984.

Chiang, Y., D. P. Birnie III, and **W. D. Kingery,** *Physical Ceramics,* John Wiley & Sons, Inc., New York, 1997.

Cullity, B. D., and **S. R. Stock,** *Elements of X-Ray Diffraction,* 3rd ed., Prentice-Hall, Upper Saddle River, NJ, 2001. A revision of a classic text and an especially clear discussion of the principles and applications of x-ray diffraction.

Wyckoff, R.W. G., Ed., *Crystal Structures,* 2nd ed., Vols. 1–5 and Vol. 6, Parts 1 and 2, John Wiley & Sons, Inc., New York, 1963–1971. An encyclopedic collection of crystal structure data.